Cross-layer Design for the Transmission of Multimedia Traffic over Fading Channels

By Tahmid Al-Mumit Quazi

Submitted in fulfilment of the academic requirements
for the degree of Doctor of Philosophy in Engineering
in the Faculty of Engineering
at the University of KwaZulu-Natal, Durban, South Africa

December 2009

As the candidate's supervisor I have approved this dissertation for submission.

Signed: _____

Name: Professor HongJun Xu

Date: 15 December 2009

Declaration

I, Tahmid Al-Mumit Quazi, declare that

i. The research reported in this thesis, except where otherwise indicated, is my original work.

ii. This thesis has not been submitted for any degree or examination at any other university.

iii. This thesis does not contain other persons' data, pictures, graphs or other information, unless specifically acknowledged as being sourced from other persons.

iv. This thesis does not contain other persons' writing, unless specifically acknowledged as being sourced from other researchers. Where other written sources have been quoted, then:

   a. their words have been re-written but the general information attributed to them has been referenced;

   b. where their exact words have been used, their writing has been placed inside quotation marks, and referenced.

v. Where I have reproduced a publication of which I am an author, co-author or editor, I have indicated in detail which part of the publication was actually written by myself alone and have fully referenced such publications.

vi. This thesis does not contain text, graphics or tables copied and pasted from the Internet, unless specifically acknowledged, and the source being detailed in the thesis and in the References sections.

Signed:

Acknowledgements

I would like to sincerely thank my supervisor, Professor HongJun Xu, who has been my teacher, guide and companion on the long journey to complete the work for this thesis. His passion for research and his persistent support and encouragement for his students is extraordinary. I feel thankful that I have had the opportunity to stand on the shoulders of a giant. Many thanks go the Telkom Centre for Radio Access Technologies at the School of Electrical, Electronic and Computer Engineering for their initial support for this project.

I would like to thank my family and friends for their encouragement and support through the difficult times. I would like to thank my parents in particular for their kind sacrifices as they will their children on to progress in their lives. I would also like to thank my 'family' at the Wu-Shin Chi Dao Foundation. The attitudes I develop from my interaction with such kindred spirits pushes me to continuously strive for the best.

Abstract

Providing guarantees in the Quality of Service (QoS) has become essential to the transmission of multimedia traffic over wireless links with fading channels. However this poses significant challenges due to the variable nature of such channels and the diverse QoS requirements of different applications including voice, video and data. The benefits of dynamic adaptation to system and channel conditions have been accepted, but the true potential of optimized adaptation is lost if the layers operate independently, ignoring possible interdependencies between them. Cross-layer design mechanisms exploit such interdependencies to provide QoS guarantees for the transmission of multimedia traffic over fading channels.

Channel adaptive M-QAM schemes are examples of some of the earliest works in the area of cross-layer design. However, many of the original schemes use the assumption that thresholds designed for AWGN channels can be directly applied to slow-fading channels. The thresholds are calculated with a commonly used approximation bit error rate (BER) expression and the first objective of the thesis was to study the accuracy of this commonly used expression in fading channels. It is shown that that the inaccuracy of the expression makes it unsuitable for use in the calculation of the threshold points for an adaptive M-QAM system over fading channels. An alternative BER expression is then derived which is shown to be far more accurate than the previous one. The improved accuracy is verified through simulations of the system over Nakagami-*m* fading channels.

Many of the cross-layer adaptation mechanisms that address the QoS provisioning problem only use the lower layers (physical and data link) and few explore the possibility of using higher layers. As a result, restrictions are placed on the system which introduces functional limitations such as the inability to insert more than one class of traffic in a physical layer frame. The second objective in this thesis was to design a physical and application layer cross-layer adaptation mechanism which overcomes this limitation. The performance results of the scheme in both AWGN and fading channels show that the cross-layer mechanism can be efficiently utilized for the purposes of providing error rate QoS guarantees for multimedia traffic transmissions over wireless links.

Contents

List of Figures

List of Tables

List of Acronyms

3G	Third Generation
AMC	Adaptive modulation and coding
ARQ	Automatic repeat request
AWGN	Additive white Gaussian noise
BER	Bit error rate
BPSK	Binary phase shift keying
CDMA	Code division multiple access
CRC	Cyclic redundancy check
CLD	Cross-layer design
CSI	Channel state information
DF	Decode and forward
DSSC	Distributed switch and stay combining
EG	Equal gain
FDM	Frequency division mode
FEC	Forward error correction
FIFO	First-in-first-out
FTP	File transfer protocol
IEEE	Institute of Electrical and Electronic Engineers
LAN	Local area network
MAC	Medium access control
MAN	Metropolitan area network
MIMO	Multiple-input-multiple output
ML	Maximum-likelihood
MR	Maximal ratio
OFDM	Orthogonal frequency division multiplexing
OSI	Open systems interconnections
PAN	Personal area network
PER	Packet error rate
QAM	Quadrature amplitude modulation
QoS	Quality of service
RS	Reed-Solomon
SC	Selection combining
SER	Symbol error rate
SNR	Signal-to-noise ratio
SSC	Switch and stay combining
TDM	Time division multiplexing
TDMA	Time division multiple access
UEP	Unequal error protection
VoIP	Voice over IP
WiMAX	Worldwide Interoperability for Microwave Access

WLAN Wireless local area network

Chapter 1

Introduction

1.1 Background

The proliferation of the Internet and broadband wireless access has made the vision of any-time, any-where computing and communication a reality. Today wireless access is available in the form of PANs (personal area networks e.g. using Bluetooth), LANs (local area networks e.g. using IEEE 802.11), MANs (metropolitan area networks e.g. using IEEE 802.16) or in the form of current 3G cellular networks. There has also been a surge in the number and type of applications that can be run over wireless networks. Multimedia applications such as videoconferencing, emergency services, surveillance, telemedicine, remote teaching and learning have been added to traditional uses of the Internet such as Voice over IP (VoIP), video streaming and data transmission through e-mail, file transfers (FTP) and web browsing. Guaranteeing quality of service (QoS) for the transmission of multimedia traffic is vital if these applications are to receive wide spread acceptance. The salient QoS requirements of such multimedia applications are high bandwidth, low delay and loss-tolerance, and these vary significantly from application to application. Achieving this in the wired environment, with its high resource availability, is not as much of a challenge as in the wireless environment where the resources are relatively very limited. The problem in the wireless networks becomes exacerbated when users expect a similar QoS from the wireless access as they experience in the wired networks.

The following factors make the greatest difficulty in providing QoS guarantees in wireless/mobile network as compared to wired networks:

- The amount and quality of resources available in wireless networks are scarce when compared to wired networks. The resources include bandwidth and the number of users the network can accommodate simultaneously.
- Wireless channels are far less reliable than channels on wired networks and are susceptible to errors due to noise, multipath fading, shadowing and interference.
- The mobility in wireless networks not only create problems such as multipath interference, but also cause mobility hand-off problems that need to be solved.

Thus there has been significant research and development effort in the area of multimedia QoS provisioning in order to improve the quality of experience that the user gets from the use of wireless networks while enjoying facilities such as mobility and roaming. A novel methodology in this research effort called cross-layer design has received a great deal of interest recently and is presented in the next section.

1.2 Cross-layer design

The classical approach to solving the problem of guaranteeing QoS in wireless networks has been to adapt existing wired algorithms and protocols for multimedia transmission to the rapidly varying and scarcely resourced wireless networks [1]. This has resulted in importing the paradigm of the OSI (open systems interconnection) layered structure in the transmission of data. In this structure each layer of the stack optimizes its performance by adapting its parameters to varying network conditions and thus providing its best service to adjacent layers. The solutions developed in this paradigm however do not take into consideration the various characteristics of multimedia traffic. This type of optimization leads to simple independent implementations of the protocol layers, but results in suboptimal performance for multimedia transmissions in wireless links.

In order to break out of the strict layered architecture paradigm, researchers recently have been viewing the protocol layers as *interdependent* as opposed to isolated, *independent* operations. In this view the interdependence is exploited such that there is a high level of information sharing between the layers so that the system as a whole can be optimized to perform more effectively and efficiently. This has led to the development of the research area broadly referred to as cross-layer design. The general objective of the research is to develop an integrated framework for jointly analysing; selecting and adapting the different strategies available at the various OSI layers in order to improve the performance of multimedia transmissions over wireless networks.

1.3 Classification of cross-layer solutions

To gain an overview of the principles that direct currently proposed cross-layer designs the following classification is presented in [1]:

- **Top-down approach** – In the schemes that fall in this category, a higher layer protocol optimizes its parameters and then the strategies at the layer below it. An example of this would be a case where the application layer dictates the MAC

parameters and strategies and MAC has to select its parameters and operation accordingly.

- **Bottom-up approach** – In these schemes the lower layers try to protect the higher layers from losses and channel variations. This solution is not always optimal for multimedia transmission due to the resulting delays and throughput variations.
- **Application-centric approach** – The application layer optimizes each lower layer parameter consecutively in either a top-down or bottom up manner based on its requirements. However, there are efficiency limitations in such an approach because the application layer operates at slower timescales and coarser data granularities than the lower layers and is not able to instantaneously adapt its performance.
- **MAC-centric approach** – In this approach the MAC layer receives the application layer's traffic information and requirements. The MAC then is responsible for deciding which application layer packets should be transmitted and for selecting the physical layer parameters based on the available channel information.
- **Integrated approach** – The strategies of the various layers are determined jointly in this approach. However, trying all possible strategies and parameters in the interacting layers in order to choose a composite strategy which will lead to the optimum system performance results in a complex cross-layer optimization problem which may not always be practical.

The above cross-layer design approaches have different advantages and disadvantages and the optimum solution depends on the application, complexity and power requirements of the multimedia transmission system being implemented. The application of cross-layer design for QoS provisioning is discussed in the next section.

1.4 QoS provisioning with cross-layer design

An excellent review of the challenges, principles and proposed schemes for improving QoS in multimedia applications through cross-layer strategies has been provided in [1]. Cross-layer design has been used to design resource allocation algorithms for multimedia QoS guarantees in [2-12]. The radio resources managed at the physical and data link layers in the work in [2] were frequency bands and bandwidth. In addition, the scheme in [2] performed scheduling of users at the MAC layer depending on each user's channel quality. The cross-layer resource allocation scheme in [3] tackled the problem of packet dropping during a hand-off. Call-admission control and resource reservation mechanisms were used at the data link layer to allocate resources adaptively to real-time service classes with stringent delay

bounds. The system in [3] also accommodated adaptive multimedia applications at the application layer to further reduce blocking and dropping probabilities. The work in [4] proposed a suite of cross-layer design modules for multimedia QoS guarantees. The suite included priority admission control which admitted users depending on their QoS profiles, a resource allocation module which allocated optimum combination of all system parameters and a scheduling mechanism which aimed at achieving better overall throughput gain and guaranteed the QoS requested by different users' service levels. The adaptive resource allocation scheme in [6] combined a truncated ARQ at the data link layer with an adaptive modulation and coding (AMC) at the physical layer to optimize the system performance for QoS guaranteed traffic. The dynamic resource allocation scheme in [9] was proposed for an orthogonal frequency division multiplexing (OFDM) system transmitting traffic with heterogeneous delay constraints. The resource allocation in [9] was based on the users' channel information at the physical layer, source statistics at the application layer and delay requirements of each class of traffic. The scheme in [10] is also based on an OFDM system but the resources managed in the scheme were sub-carriers and transmission power. The scheme in [11] is based on a multiple-input-multiple-output OFDM (MIMO-OFDM) wireless network and combined an adaptive physical and MAC layer. At the physical layer the dynamic resource allocation algorithm in [11] adaptively allocated transmit antennas and modulation levels for real and non-real time traffic to increase the system spectral efficiency while guaranteeing distinct BER-QoS requirements. At the MAC layer the scheme dynamically assigned time-slots for real-time users in a time division mode (TDM) to guarantee bounded delays while adaptively allocating sub-carriers for non-real time traffic in frequency division mode (FDM) to maximize the system throughput. The work in [12] proposed a scheme for the transmission of multimedia traffic with diverse QoS requirements for a WiMAX system. The cross-layer design was aimed at maximizing the system throughput while satisfying diverse QoS requirements by jointly designing packet scheduling, sub-carrier allocation and adaptive modulation and coding.

The cross-layer design approach was used to develop scheduling schemes for multimedia QoS provisioning in [13-18]. Generally, the schemes combined a channel adaptive module at the physical and data link layer with a traffic aware scheduling scheme at the MAC layers with the objective of guaranteeing multimedia QoS while improving system performance in terms of metrics such as fairness and throughput.

Most of schemes referenced above used a combination of the physical, MAC and data link layers. The common thread between the cross-layer designs in [19-21] was that the schemes

used the application layer in conjunction with the lower layers. In [19] the source code rate at the application layer, congestion control at the transport layer were jointly designed to reduce throughput degradation caused by the transmission errors of the wireless channel and to support the QoS requirements of the video streaming application. In a similar scheme in [20], the scheme abstracted parameters at the application layer to describe the rate-distortion characteristics of the pre-encoded video streams. At the lower layers the abstracted parameters described the current transmission characteristics of each user. Then joint optimization of these layers were performed to propose an adaptive resource allocation scheme at the physical and data link layers and a decision making mechanism at the application layer to determine which frames to send in the next transmission. The cross-layer scheme in [21] was designed for the transmission of scalable video transmissions over 3rd Generation (3G) wireless networks. The scheme took into consideration the time-varying channel/network conditions and scalable video codec characteristics to allocate resources between the source and channel coders based on a minimum distortion and minimum power criterion. A hybrid unequal error protection (UEP) was used at the application layer source coder and an adaptive delay constrained automatic repeat request (ARQ) was used at the data link layer.

In summary, if the classification presented in the previous section is used, it can be observed that the cross-layer schemes in [13-18] used a MAC-centric approach, those in [19-21] used an application-centric approach while the schemes in [2-12] used the integrated approach to combine various layers to guarantee QoS targets while meeting some particular objective. The application-centric bottom-up approach is used further on in this thesis where the concept of combining an unequal error protection scheme at the application layer with a channel adaptive scheme at the lower layers is used to design a novel cross-layer scheme to guarantee QoS targets (in terms of packet error rate (PER)) for multimedia traffic.

1.5 Main contributions

The main contributions of this thesis are as follows:

- The thesis re-addressed the method used to determine the switching thresholds for an adaptive M-QAM scheme used in the AMC module of a cross-layer design operating in a fading channel. QAM here stands for quadrature amplitude modulation, and M represents the QAM modulation mode, and thus the number of bits per symbol, used by the AMC module. It is first shown that an approximate BER expression for M-QAM commonly used in literature for determining the

system thresholds and average BER performance in a fading channel leads to significant inaccuracies. Alternative BER expressions for M-QAM in additive white Gaussian noise (AWGN) are then derived and used to improve the accuracy of the adaptive M-QAM system design in Nakagami-m fading channels. The accuracy improvement in the theoretical design is verified via simulations.

- A novel physical and application layer cross-layer scheme is proposed that aims to provide error rate QoS guarantees for multimedia traffic transmissions over wireless channels. The proposed system facilitates a more efficient dynamic resource allocation where more than one class of traffic can be transmitted simultaneously in a physical layer frame. The theoretical performance of the cross-layer design is verified through system simulations in AWGN and Nakagami-m fading channels.

1.6 Organization of the thesis

The remainder of the thesis is organized as follows.

The accuracy of a commonly used approximate BER for M-QAM in a fading channel is investigated in Chapter 2. The inaccuracy of the approximate expression is demonstrated via accurate simulations over a slowly varying Nakagami-m block-fading channel. It is also shown that threshold points for an adaptive M-QAM system, given a target BER, determined using the approximate BER expression lead to inappropriate operation of the system in a fading channel.

In Chapter 3, two alternative approximate BER expressions for M-QAM in AWGN are derived and used to calculate the average BER of M-QAM over a Nakagami-m fading channel. The new average BER expressions are shown to be far more accurate than the commonly used method discussed in Chapter 2. The threshold values for the adaptive M-QAM system are then determined using one of the average BER expressions and simulation results are presented to show the accuracy of the new threshold points.

Chapter 4 discusses a few cross-layer design mechanisms for QoS provisioning for multimedia traffic and highlights a functional limitation in most of the schemes in that only a single class of traffic can be transmitted in a physical layer frame. The motivation for overcoming this limitation is then discussed.

A novel physical and application layer cross-layer design mechanism is proposed in Chapter 5 which overcomes the limitation discussed in Chapter 4. A detailed system design is

presented and verified through simulations in the AWGN channel. Using the more accurate physical layer adaptive M-QAM scheme proposed in Chapter 3, the cross-layer design in Chapter 4 is re-designed for operation in a Nakagami-m fading channel and this is presented in Chapter 6. System simulations in the fading channel are once again used to verify the theoretical design.

Chapter 7 concludes the thesis and discusses possible future research directions.

This work has been presented in the following publications:

Quazi T., Xu H., Takawira F., "QoS Provisioning using Cross-Layer Design", In Proceedings of Southern African Telecommunications Networks and Applications Conference (SATNAC), ISBN 978-0-620-39352-5, Mauritius, Sep. 2007.

Quazi T., Xu H., Takawira F., "Quality of Service for Multimedia Traffic using Cross-Layer Design", *IET Communications Journal*, vol 3, issue 1, pp 83-90, Jan. 2009.

Quazi T., Xu H., "Performance Analysis of Adaptive M-QAM over a Flat Fading Nakagami-m Channel," [Prepared for submission to *IET Communications Journal*]

Chapter 2

Review of adaptive M-QAM

2.1 Introduction

One of the earliest contributions in the research area of cross-layer design was to increase the spectral efficiency of transmissions by adapting certain parameters of the signal to match the wireless channel conditions. Physical and data link layers were combined to allow the adaptive variation of the transmission power, symbol rate, channel coding rate, constellation size or any combination of these parameters. Channel adaptive M-QAM schemes have been proposed which provide higher average link efficiency by taking advantage of the time-varying nature of wireless fading channels: transmitting data using high modulation schemes when the channel is good, and smoothly moving to lower modulation schemes as the channel degrades. Much of the earlier work on such schemes uses the assumption that thresholds for adaptive M-QAM designed for AWGN channels can be directly applied to slowly varying block fading channels. This is done assuming that the channel signal-to-noise ratio is approximately constant in each bin [28]. The thresholds are calculated with a commonly used approximate bit error rate (BER) expression in these schemes. In this chapter the first aim is to study this commonly used expression and investigate the accuracy of its use to derive the average BER of M-QAM in a fading channel. This is done by comparing the result of the average BER expression derived using the approximate expression with results of simulations over a Nakagami-m block fading channel. The second aim in the chapter is to show that the inaccuracy in the threshold values determined using the closed form approximation expression will lead to inappropriate operation of the adaptive M-QAM scheme in a fading channel. This is done by comparing expected theoretical values with the simulation results. The accuracy of the adaptive M-QAM in a fading channel is investigated in this chapter because it is used in the adaptive modulation and coding (AMC) module of a cross-layer design proposed later in the thesis, and the accuracy of the AMC module is essential to scheme's operation.

2.2 Related work

Discrete-rate M-QAM has been applied to various channel adaptive transmission schemes [22-36]. The objective of all of these schemes is to enhance the spectral efficiency of the transmissions by using M-QAM to adapt the transmission rate to a time-varying fading channel. The work in [22-24] demonstrated the improvement in spectral efficiency of the adaptive system while achieving a specified QoS bit error rate (BER) target in the operable signal-to-noise ratio (SNR) range. The work in [25-28] further improved the performance of the adaptive system by combining coding with rate adaptive M-QAM. The work in [29-31] used an adaptive M-QAM and coding system in the physical layer module of the cross-layer design mechanisms. The work in [29-30] combined the adaptive physical layer with the data link layer while in [31] it was combined with the application layer. The work in [32-35] combined M-QAM adaptive modulation to diversity combining to propose schemes where the modulation mode and the diversity combiner structure are adaptively determined based on the channel fade condition and the error-rate requirement. The work in [36] analyzes the performance of an amplify and forward cooperative system with constant-power, rate-adaptive M-QAM transmission.

In the system design and performance analysis in most of the works referenced above [22, 24-33, 31-33, 35-36], the derivation of the system BER has been done using a common approximate expression for BER of M-QAM in AWGN [22, eq 3]. This expression is used to derive the average BER expression for the performance analysis of these systems in a fading channel. Additionally, this simple closed form BER expression has been used to determine the SNR boundaries of the adaptive system. The assumption of all the works in [22-36] is that the threshold values, determined using an AWGN BER expression, can be used for the adaptive system in a fading channel because slowly fading block fading channels can be modelled as AWGN channels. This follows from the assumption that the channel signal-to-noise ratio is approximately constant within each bin [28]. Most of these works referenced above presented the BER performance of the system over Nakagami-m fading channel using only theoretical analysis and did not verify the system design using simulations, and only the work in [24] has presented system simulations. Although [24] is an exception, the performance curves show that there is a significant gap between the analytical expression and the simulation result. The authors of [24] explain that gap exists as a result of choosing overly conservative design values for the threshold points. The authors in [36] also confirm this statement and mention that the threshold can be further optimized. The motivation for the work in this chapter is to investigate the accuracy of using the common BER expression

for deriving the average BER of M-QAM in a fading channel and the accuracy of the assumption that threshold values designed for AWGN channels can be used in Nakagami-m fading channels.

2.3 Approximate BER expression

The adaptive schemes in [22, 24-33, 31-33, 35-36] use the approximation expression for BER of coherent M-QAM with two-dimensional Gray coding over the AWGN channel [22, eq. 3] given by

$$P_b(\gamma) \cong 0.2exp\left(\frac{-3\gamma}{2(M-1)}\right), \tag{2.1}$$

where M represents the M-QAM modulation, γ is the received signal-to-noise ratio (SNR) per symbol. The authors of [25] motivate the use of the above expression because it is an upper bound on the BER performance of M-QAM for M $\geq$ 4 and because it is "invertible" in the sense that it provides a simple closed-form expression to determine the BER of an M-QAM modulation given a SNR value

$$\gamma = \frac{2}{3}K_0(M-1), \tag{2.2}$$

where $K_0 = -ln(5BER)$.

2.4 Average BER of M-QAM in a Nakagami-m fading channel

2.4.1 Fading channel model

In transmissions over Nakagami-m fading channels, at the receiver, the received signal is given by $r = \alpha t + n$ where α is the Nakagami-m fading channel gain, t is the transmitted signal and n is the additive white Gaussian noise which has a zero-mean and a variance of N_0, where N_0 is the single sided power spectrum density of the noise. The probability density function (pdf) of the Nakagami-m fading channel gain (α) is given by (2.3)

$$p_\alpha(\alpha) = \frac{2}{\Gamma(m)}\left(\frac{m}{\Omega}\right)^m \alpha^{2m-1} exp\left(-\frac{m}{\Omega}\alpha^2\right), \tag{2.3}$$

where m is the Nakagami fading parameter and $\Gamma(m)$ is the gamma function defined by $\Gamma(m) = \int_0^\infty y^{m-1} exp(-y)dy$ and $\Omega = E[|\alpha|^2]$, E being the expectation. Define the received instantaneous SNR as $\gamma = \frac{|\alpha|^2 E_s}{N_0}$ (E_s is the symbol energy). For a Nakagami-m fading channel, then the pdf of γ is given by [22]:

$$p_\gamma(\gamma) = \left(\frac{m}{\bar{\gamma}}\right)^m \frac{\gamma^{m-1} exp\left(-\frac{m\gamma}{\bar{\gamma}}\right)}{\Gamma(m)}, \gamma \geq 0, \tag{2.4}$$

where

$$\bar{\gamma} = E[\gamma] = \Omega\frac{E_s}{N_0}. \tag{2.5}$$

The average BER of M-QAM in a slow flat Nakagami-m fading channel may be derived by averaging the error rates for the AWGN channel (2.1) over the range of the SNR in Nakagami-m fading:

$$\begin{aligned} P_b(\bar{\gamma}) &= \int_0^\infty P_b(\gamma) \times p_\gamma(\gamma)d\gamma \qquad (2.6)\\ &= \int_0^\infty 0.2exp\left(\frac{-3\gamma}{2(M-1)}\right) \times \left(\frac{m}{\bar{\gamma}}\right)^m \frac{\gamma^{m-1} exp\left(-\frac{m\gamma}{\bar{\gamma}}\right)}{\Gamma(m)} d\gamma \\ &= \frac{0.2}{\Gamma(m)}\left(\frac{m}{\bar{\gamma}}\right)^m \int_0^\infty \gamma^{m-1} exp(-\gamma\beta)d\gamma, \end{aligned}$$

where $\beta = \frac{3\bar{\gamma}+2m(M-1)}{2(M-1)\bar{\gamma}}$, and $\bar{\gamma}$ is the average SNR per symbol defined in (2.5). After completing the integration (refer to Appendix I) and some simplification the expression for the average BER can be derived as

$$P_b(\bar{\gamma}) = 0.2\left(\frac{m}{\bar{\gamma}\beta}\right)^m. \quad (2.7)$$

2.4.2 Simulation of Nakagami-m channels

In order to investigate the accuracy of (2.7), the system needed to be simulated over the Nakagami-m fading channel. Recently a novel procedure for the generation of accurate Nakagami-m processes with arbitrary values of $m \geq 0.5$ was presented in [38-39]. The author cites previous works, including [37], none of which presents schemes capable of generating Nakagami-m processes with accurate phase statistics. The key contribution in [38] is a technique referred to as *random mixture* in which the Nakagami-m process is generated not by adding, but rather by *drawing* from (or *mixing*) a pair of different Nakagami-m processes. The technique is mathematically founded on known properties of Nakagami-m processes and its corresponding proofs and derivations can be found in [38].

Using the technique in [38], M-QAM, with $M = 16, 32, 64$ and 128 was simulated over $m = 1$ and $m = 2$ Nakagami-m fading channels and compared to the theoretical results obtained from using the approximate average BER expression (2.7). The first point of note is the gap between the simulation and theory graphs for all four modulation schemes. For purposes of clarity only the graphs for $M = 16$ and 128 are shown in Figure 2-1 and Figure 2-2 for $m = 1$ and $m = 2$, respectively. As the graphs show, there is a significant difference (a gap of up to 4dB) between the average BER computation using (2.7) and the simulation for 128-QAM. The gap increases as M increases. We propose that the major reason for the performance difference between the simulation curve in [24] (and the 'exact' curve in [22]) and the analysis of the rate adaptation scheme is the inaccuracy of the expression in (2.7). Even though the gap for 16-QAM appears small, it will contribute to the inaccuracies in the operation of the adaptive M-QAM system in a Nakagami-m fading channel, which will lead to the inappropriate operation of the adaptive system in such a channel.

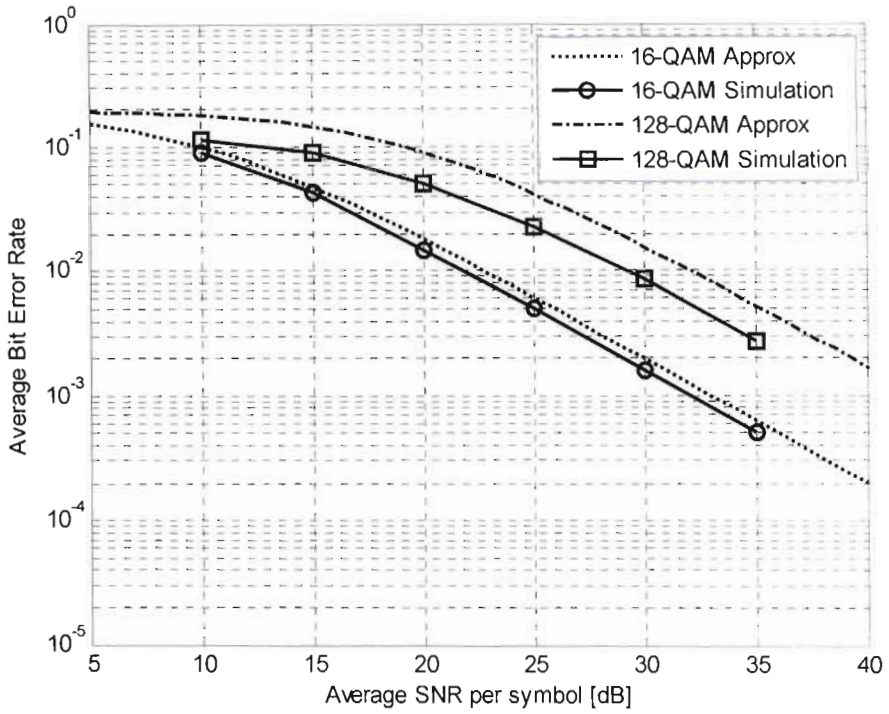

Figure 2-1: Average BER of M-QAM over an $m = 1$ Nakagami-m fading channel using the approximation BER expression (2.7)

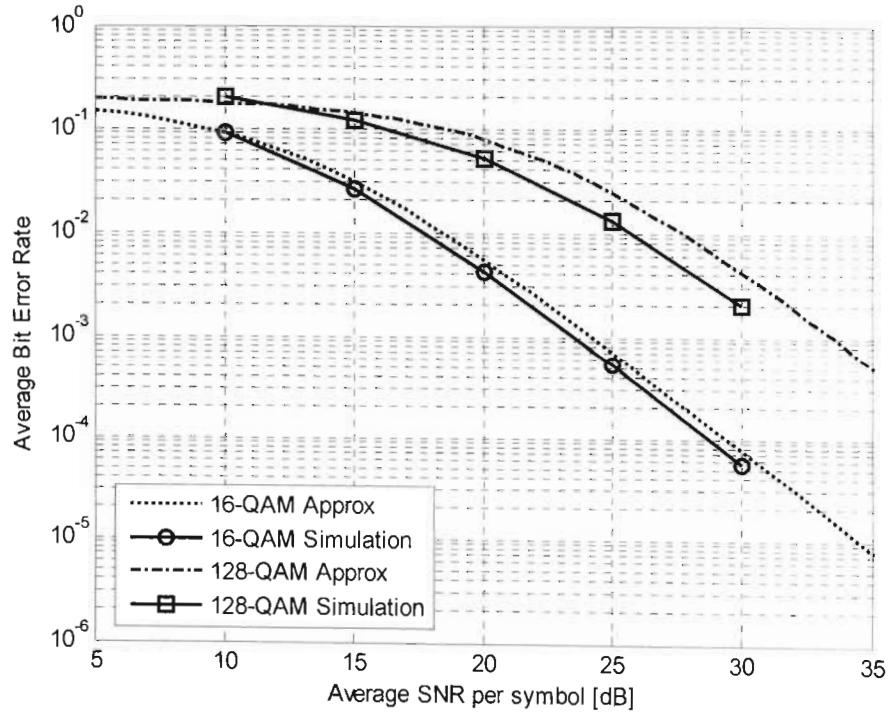

Figure 2-2: Average BER of M-QAM over an $m = 2$ Nakagami-m fading channel using the approximation BER expression (2.7)

The effect of varying the Nakagami m parameter is shown in Figure 2-3, where the theory and simulation curves for 128-QAM is plotted for the $m = 1$ and $m = 100$ Nakagami-m fading channels. The graphs show that as the value of the m parameter increases the gap decreases. Thus when $m = \infty$, the fading channel would resemble the Gaussian channel and the gap would be considerably smaller, however for smaller values of m, such as $m = 1$ which corresponds to Rayleigh fading, the gap is significant as shown in Figure 2-3.

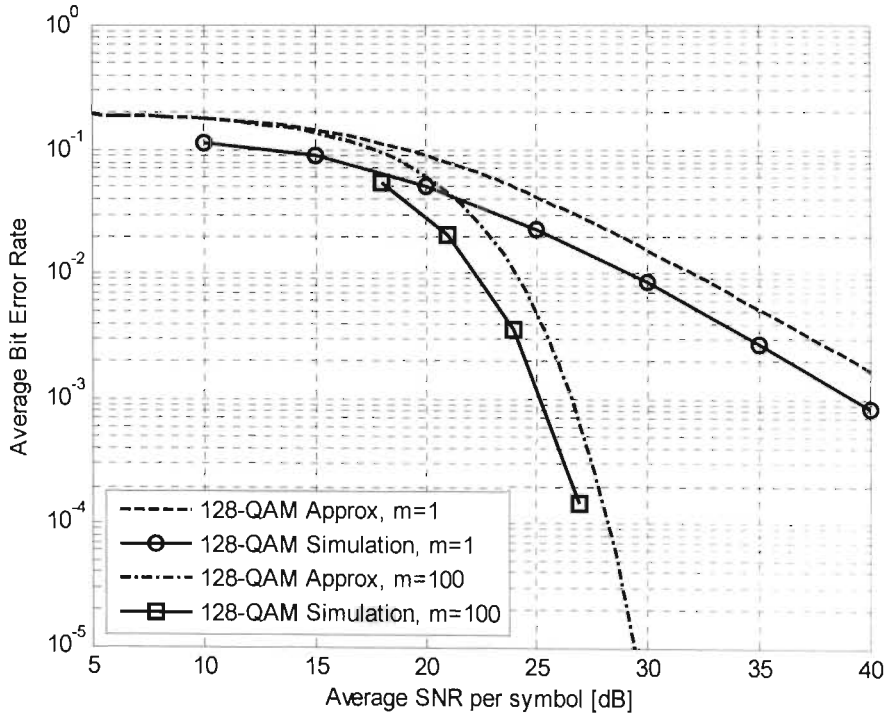

Figure 2-3: Average BER of 128-QAM over $m = 1$ and $m = 100$ Nakagami-m fading channels

2.5 Adaptive M-QAM modulation

A block diagram of the channel adaptive M-QAM system is shown in Figure 2-4 [24].

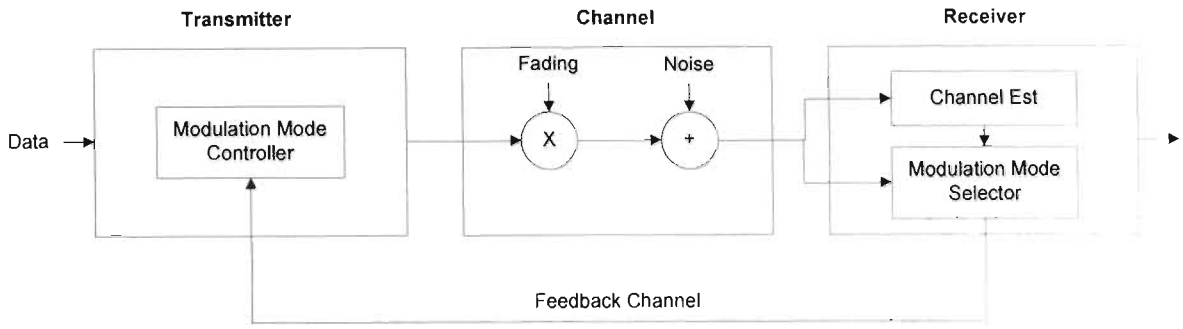

Figure 2-4: Adaptive M-QAM system model [24]

In the modulation mode controller of Figure 2-4, Gray coded discrete (square and rectangular) M-QAM modes with $M := 2^n (n = 1, 2, 3, \dots, N)$ are used for the channel adaptive scheme. The transmissions are assumed to be over a slowly varying flat fading channel with the fading assumed to follow a Nakagami-m distribution. This corresponds to a block fading model where the rate adjustment occurs on a frame-by-frame basis. The signal at the receiver is perturbed by an additive white Gaussian noise (AWGN) which is modeled as a zero-mean complex Gaussian random variable with variance $N_0/2$ per dimension, where N_0 is the single sided power spectrum density of the noise. It is assumed that perfect channel estimation is possible at the receiver, and that the feedback channel is instantaneous and error free.

The received SNR range is split into $(N + 1)$ fading regions (bins), with region n having a corresponding mode n. The set $\{\gamma_n\}_{n=1}^{N}$ contains the lower thresholds for the N fading regions, calculated such that the target BER (referred to as BER_0) is achieved for each M-QAM modulation scheme. γ_0 is set to 0 and γ_{N+1} to ∞. Thus when the received instantaneous SNR, γ, falls within region n ($\gamma_n \leq \gamma < \gamma_{n+1}$), the associated fading index n is sent back to the transmitter through a dedicated feedback channel. To avoid deep fades, no data is sent when $\gamma_0 \leq \gamma < \gamma_1$ (outage).

In the proposed scheme in [22], if a target BER is set to BER_0, the region boundaries (or switching thresholds) $\{\gamma_n\}_{n=1}^{N}$ are set to the SNR required to achieve the target BER_0 using M-QAM over an AWGN channel. Specifically,

$$\gamma_1 = [erfc^{-1}(2BER_0)]^2; \text{ for BPSK} \tag{2.8}$$

$$\gamma_n = \frac{2}{3} K_0 (2^n - 1); \quad n = 2, 3, \dots, N; \text{ for M-QAM} \tag{2.9}$$

$$\gamma_{N+1} = +\infty \tag{2.10}$$

where $K_0 = -ln(5BER_0)$, $erfc^{-1}$ denotes the inverse complementary error function which is defined as shown in (2.11) [43].

$$erfc(x) \triangleq \frac{2}{\sqrt{\pi}} \int_x^{\infty} e^{-t^2} dt \tag{2.11}$$

It should be noted that all the γ_ns (except for γ_1) are chosen according to the approximation BER expression (2.1). Since (2.1) is an upper bound of the BER only for M $\geq$ 4, γ_1 is chosen according to the exact BER performance of BPSK.

If BER_0 is set to 1×10^{-3}, the switching thresholds for adaptive M-QAM using (2.8) – (2.10) are given in Table 2-1. R_n is the bits per symbol for mode n.

Table 2-1: Boundary points for adaptive M-QAM modulation, for $BER_0 = 1 \times 10^{-3}$

Mode (n)	1	2	3	4	5	6	7
M	BPSK	4QAM	8QAM	16QAM	32QAM	64QAM	128QAM
SNR(dB)	6.79	10.25	13.93	17.24	20.39	23.47	26.52
R_n	1	2	3	4	5	6	7

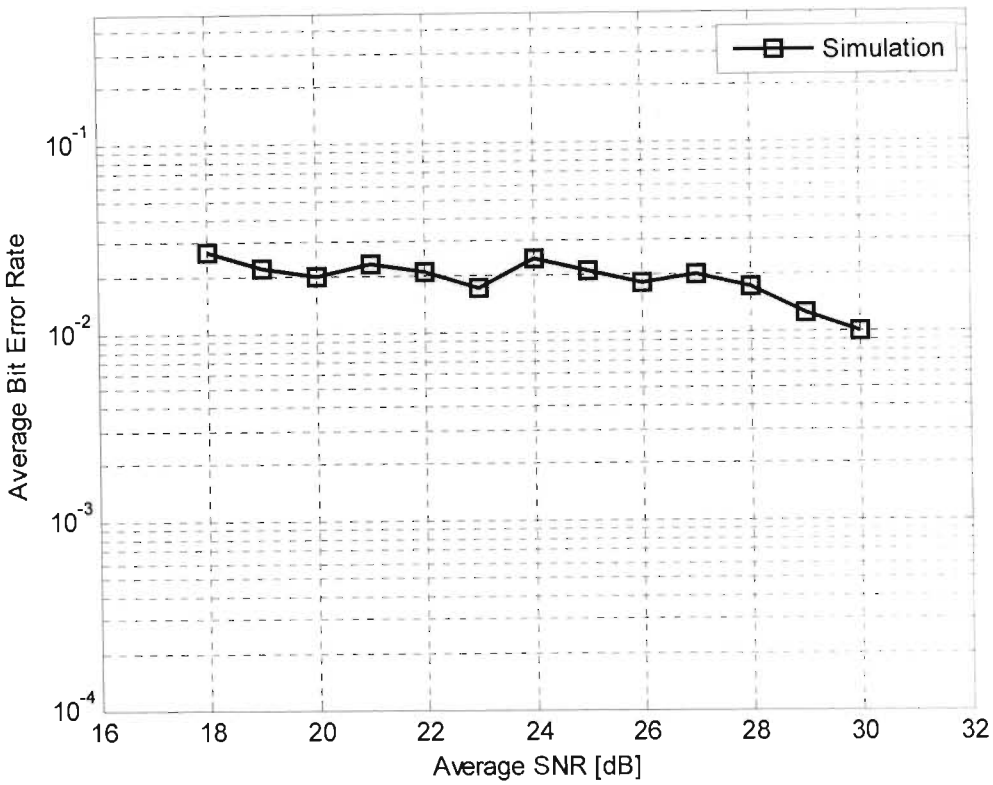

Figure 2-5: Average BER of adaptive M-QAM over an $m = 1$ Nakagami-m fading channel with thresholds calculated using the approximation BER expression (2.7)

In order to assess the accuracy of (2.1) in a fading channel, M-QAM, with $M = 16, 32, 64$ and 128 are considered. The threshold points for an adaptive M-QAM system for a target BER of 1×10^{-3} according to Table 2-1 are 17.24dB, 20.39dB, 23.47dB and 26.52dB respectively. However the simulation results for the adaptive M-QAM system for the $m = 1$ Nakagami- m fading channel in the region from 18dB to 30dB in Figure 2-5 shows that the system BER at these points would be near 2×10^{-2}, pointing to the inaccuracy of these threshold values for the fading channel. Similar discrepancies were found for Nakagami-m fading channels with other values of m. Thus given a BER target, using (2.1) for determining the thresholds for M-QAM in a fading channel would result in inaccurate operation of the adaptive M-QAM system in a fading channel.

2.6 Conclusion

This chapter investigated the accuracy of the use of a commonly used approximate BER expression for M-QAM in an AWGN channel (2.1) in a fading channel. The conclusion of

the investigation is that approximate expression displays significant inaccuracies when used in a fading channel. The objective in the next chapter is to derive an alternative average BER expression which will improve the accuracy of the of the adaptive M-QAM system in a fading channel.

Chapter 3

Alternative adaptive M-QAM design for fading channels

3.1 Introduction

The simulation results in chapter 2 showed that using the approximate expression (2.7) will result in inaccuracies in an adaptive M-QAM modulation scheme over a Nakagami-m fading channel. Thus the aim of this chapter is to derive a more accurate expression for the BER performance of adaptive M-QAM in a fading channel in order to improve the accuracy of the channel adaptive system.

3.2 BER for M-QAM in AWGN

The exact symbol error rate (SER) for square M-QAM (i.e. $log_2 M$ is even) in an AWGN channel is given by [40]:

$$P_s^{(even)}(\gamma) = 4\left(1-\frac{1}{\sqrt{M}}\right)Q\left(\sqrt{\frac{3\gamma}{(M-1)}}\right) - 4\left(1-\frac{1}{\sqrt{M}}\right)^2 Q^2\left(\sqrt{\frac{3\gamma}{(M-1)}}\right), \tag{3.1}$$

where M represents the M-QAM modulation, γ is the received SNR per symbol [41]. The SER for a rectangular M-QAM ($log_2 M$ is odd) is tightly bound by [40]:

$$P_s^{(odd)}(\gamma) \leq 4\left(1-\frac{1}{\sqrt{M}}\right)Q\left(\sqrt{\frac{3\gamma}{(M-1)}}\right) - 4\left(1-\frac{1}{\sqrt{M}}\right)^2 Q^2\left(\sqrt{\frac{3\gamma}{(M-1)}}\right) \tag{3.2}$$

As it was discussed in Chapter 2, (2.1) is not an accurate approximation for determining the average BER of M-QAM in Nakagami-m fading channels. This was demonstrated by showing the inaccuracy of (2.7) by comparing the theoretical results with the simulation results. In order to formulate a more accurate approximation, two methods are considered in this chapter for the evaluation of $Q(x)$ and $Q^2(x)$ functions used in (3.1). The first method used the following approximations for the two functions [42-43]:

$$Q(x) \approx \frac{1}{12} exp\left(\frac{-x^2}{2}\right) + \frac{1}{4} exp\left(\frac{-2x^2}{3}\right) \tag{3.3}$$

$$Q^2(x) \approx \frac{1}{8} exp(-x^2) \tag{3.4}$$

Applying (3.3) and (3.4) into (3.1), the SER for M-QAM in AWGN is given by:

$$P_s(\gamma) \approx a\left\{exp\left(\frac{-2b\gamma}{3}\right) + \frac{exp\left(\frac{-b\gamma}{2}\right)}{3} - \frac{a \times exp(-b\gamma)}{2}\right\} \tag{3.5}$$

where $a = \left(1 - \frac{1}{\sqrt{M}}\right)$; $b = \frac{3}{(M-1)}$ and $\gamma = \frac{E_S}{N_0}$

This is referred to as Method 1 in the rest of the chapter.

For the second method, the $Q(x)$ and $Q^2(x)$functions are defined as [41]:

$$Q(x) = \frac{1}{\pi}\int_0^{\pi/2} exp(\frac{-x^2}{2sin^2\theta})d\theta \tag{3.6}$$

$$Q^2(x) = \frac{1}{\pi}\int_0^{\pi/4} exp(\frac{-x^2}{2sin^2\theta})d\theta \tag{3.7}$$

(3.6) or (3.7) cannot be evaluated in a closed-form, however the integration can be computed using a numerical integration. The trapezoidal rule for numerical integration is given as follows:

$$\int_a^b f(x) \approx \frac{b-a}{n}\left[\frac{f(a)+f(b)}{2} + \sum_{k=1}^{p-1} f\left(a + k\frac{b-a}{n}\right)\right]$$

where p is the number of summations. Applying the trapezoidal rule to equation (3.6) the following expression is derived [42]:

$$Q_p(x) = \frac{exp\left(\frac{-x^2}{2}\right)}{4p} + \frac{1}{4p}\sum_{i=1}^{p-1} exp\left(\frac{-x^2}{2sin^2\theta_i}\right) \tag{3.8}$$

where $\theta_i = \frac{i\pi}{2p}$

$Q^2(x)$ can also be derived using a similar process and is given by [42]:

$$Q_p{}^2(x) = \frac{exp(-x^2)}{8p} + \frac{1}{4p}\sum_{i=1}^{p-1} exp\left(\frac{-x^2}{2sin^2\theta_i}\right) \tag{3.9}$$

where $\theta_i = \frac{i\pi}{4p}$

It is shown in [42] that applying a p larger than 6 results in a perfect match between the exact simulation and the numerical computation for (3.1) and (3.2). Applying (3.8) and (3.9) into (3.1), and after some simplification, the SER for M-QAM is given by:

$$P_s(\gamma) = \frac{a}{p}\left\{\frac{exp\left(\frac{-b\gamma}{2}\right)}{2} - \frac{a \times exp(-b\gamma)}{2} + (1-a)\sum_{i=1}^{p-1} exp\left(\frac{-b\gamma}{S_i}\right) + \sum_{i=p}^{2p-1} exp\left(\frac{-b\gamma}{S_i}\right)\right\} \tag{3.10}$$

where $a = \left(1 - \frac{1}{\sqrt{M}}\right)$; $b = \frac{3}{(M-1)}$; $S_i = 2sin^2\left(\frac{i\pi}{4p}\right)$ and $\gamma = \frac{E_s}{N_0}$

This is referred to as Method 2 in the rest of the chapter.

3.3 Alternative average BER derivation in Nakagami-*m* fading

The average SER over a Nakagami-m fading channel is found by averaging (3.5) and (3.10) over the pdf of the SNR in Nakagami-m fading:

$$\begin{aligned} P_s(\bar{\gamma}) &= \int_{-\infty}^{\infty} P_s(\gamma) \times p_\gamma(\gamma) d\gamma \\ &= \int_0^{\infty} P_s(\gamma) \times \left(\frac{m}{\bar{\gamma}}\right)^m \frac{\gamma^{m-1} exp\left(-\frac{m\gamma}{\bar{\gamma}}\right)}{\Gamma(m)} d\gamma \,, \end{aligned} \tag{3.11}$$

where $\bar{\gamma}$ is defined in (2.5). The evaluation of (3.11) leads to the following closed form expressions for the average SER $P_S^1(\bar{\gamma})$ and $P_S^2(\bar{\gamma})$ using Method 1 and Method 2, respectively:

$$P_S^1(\bar{\gamma}) = a\left\{\left(\frac{3m}{3m + 2b\bar{\gamma}}\right)^m + \frac{1}{3}\left(\frac{2m}{2m + b\bar{\gamma}}\right)^m - \frac{a}{2}\left(\frac{m}{m + b\bar{\gamma}}\right)^m\right\} \tag{3.12}$$

$$\begin{aligned} P_S^2(\bar{\gamma}) = \frac{a}{p}\Bigg\{&\frac{1}{2}\left(\frac{2m}{2m + b\bar{\gamma}}\right)^m - \frac{a}{2}\left(\frac{m}{m + b\bar{\gamma}}\right)^m + (1-a)\sum_{i=1}^{p-1}\left(\frac{mS_i}{mS_i + b\bar{\gamma}}\right)^m \\ &+ \sum_{i=1}^{2p-1}\left(\frac{mS_i}{mS_i + b\bar{\gamma}}\right)^m\Bigg\} \end{aligned} \tag{3.13}$$

Bit error rate, $P_b^1(\bar{\gamma})$ and $P_b^2(\bar{\gamma})$, for both Method 1 and 2 is derived from the approximate relationship given by [40]

$$P_b(\bar{\gamma}) \cong \frac{P_s(\bar{\gamma})}{k}, \tag{3.14}$$

where $k = log_2 M$ bits/symbol.

Figure 3-1 and Figure 3-2 present the plots of the same modulation schemes ($M = 16$ and 128) used in Figure 2-1 and Figure 2-2. However the $P_b(\bar{\gamma})$ is determined using Method 1 and Method 2. The graphs show that, when compared to the results in Figure 2-1 and Figure 2-2, there is a much closer match between the results from the analysis expression and the simulation. The 3 to 4dB gap for 128-QAM in Figure 2-1 has been reduced to less than 0.5dB in Figure 3-1. Thus (3.14), using either method can be more confidently used for computing the average BER of M-QAM over a Nakagami-m fading channel than (2.7).

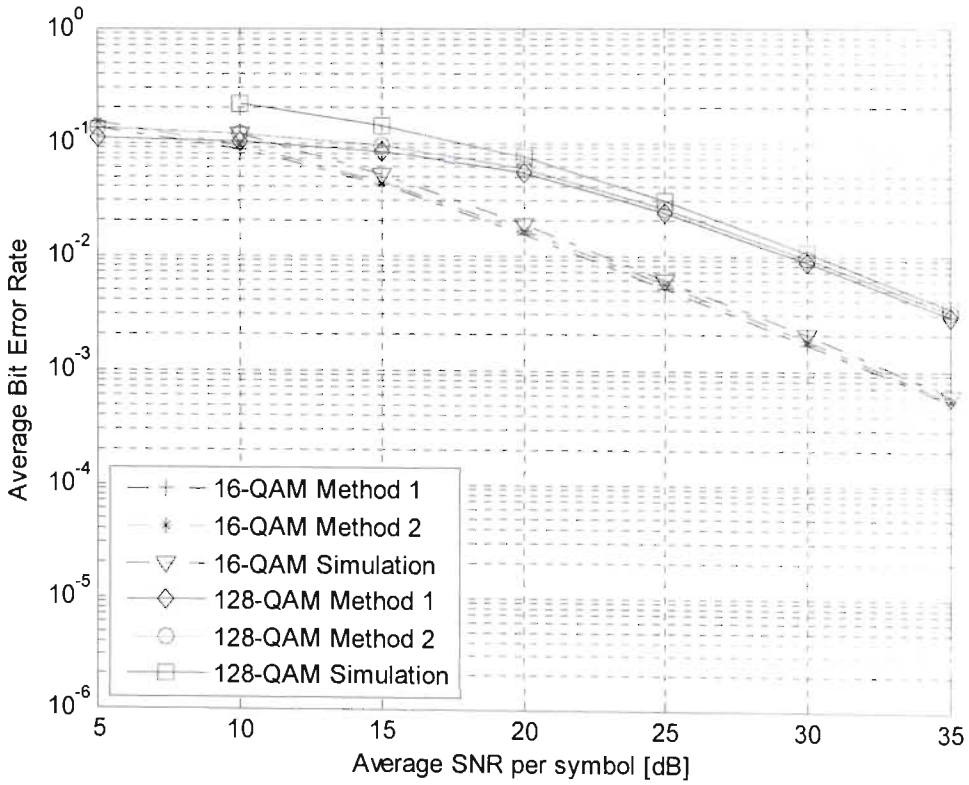

Figure 3-1: Average BER of M-QAM over an $m = 1$ Nakagami-m fading channel derived using Method 1 and Method 2

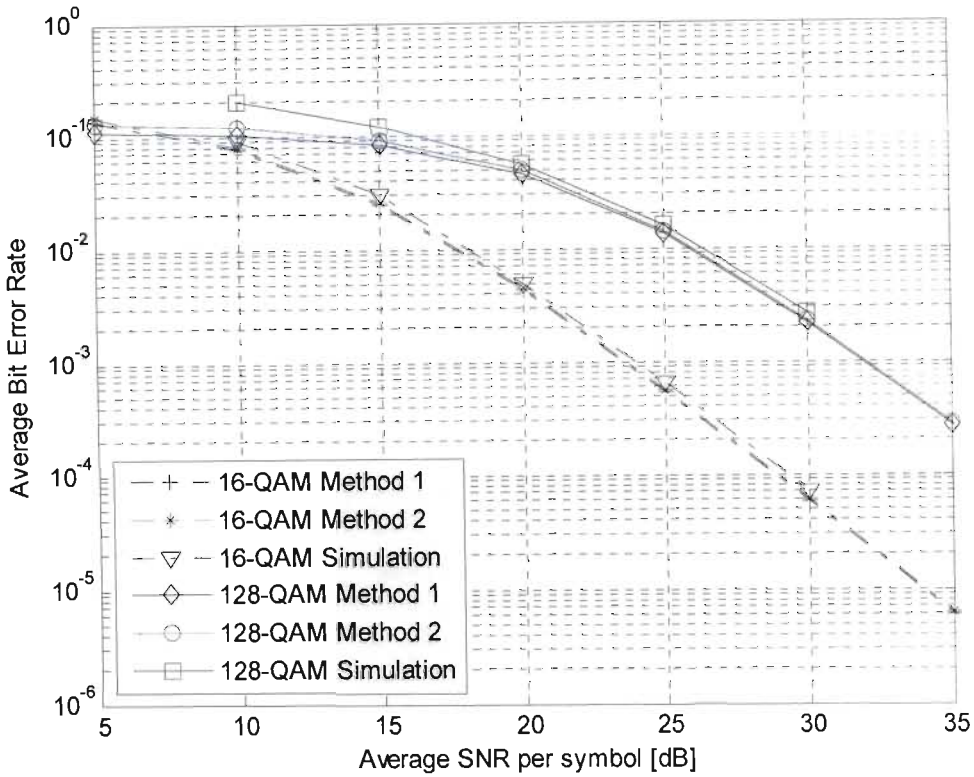

Figure 3-2: Average BER of M-QAM over an $m = 2$ Nakagami-m fading channel derived using Method 1 and Method 2

Figure 3.1 and Figure 3.2 also show a noticeable gap between the simulation and expected theoretical values for $M = 128$ in lower SNR regions (SNR < 17dB). This can be attributed to the limitation of Gray coded modulation and the approximation in (3.14) at low SNR values. The results in Figure 3.1 and Figure 3.2 show that the Gray coded modulation assertion of one symbol error equating to one bit error is upheld for high SNR values. Thus simply dividing the SER by the number of bits per symbol (k) gives an accurate BER value. However when the SNR value is low, one symbol error could be as a result of more than one bit error, and so the division by k leads to inaccuracies. This is highlighted by the plots for $M = 128$, which have higher number of bits per symbol than the other two modulation schemes. This difference between the simulation and theory curves at the lower SNR region is however ignored in the design of the adaptive M-QAM system because transmission using modulation schemes with high bits per symbol, such as 64-QAM or 128-QAM, is not considered in the low SNR regions where the BER is high. It should also be noted that Method 2 produces a slightly closer match to the simulation results when compared to Method 1.

3.4 Improved adaptive M-QAM design

The system model in this chapter is slightly modified version of that used in section 2.5 in that BPSK is no longer used. Thus the index for the set $\{\gamma_n\}_{n=2}^{N}$ now begins at 2 and γ_1 (as opposed to γ_0) is set to 0. The outage region is modified to $\gamma_1 \leq \gamma < \gamma_2$.

The next step in designing the channel adaptive M-QAM modulation scheme is to use the more accurate BER expression (3.14) to determine the SNR threshold set $\{\gamma_n\}_{n=2}^{N}$ for the Nakagami-m, $m = 1, 2\ and\ 5$, fading channel for a given QoS BER target. Due to its closer match to the simulation results Method 2 is used for the calculation of the threshold set. Using Method 2, the $P_b(\bar{\gamma})$ based on (3.14) for M-QAM, $M = 4, 8, 16, 32, 64$ and 128 over $m = 1, 2\ and\ 5$ Nakagami-m, fading channels are plotted in Figures 3-3, 3-4 and 3-5 respectively. The QoS BER target (BER_0) is set to 1×10^{-3}. Since it is not possible to get a simple BER expression which is similar to (2.1), the boundary points are determined numerically. The bin thresholds are shown in Table 3-1.

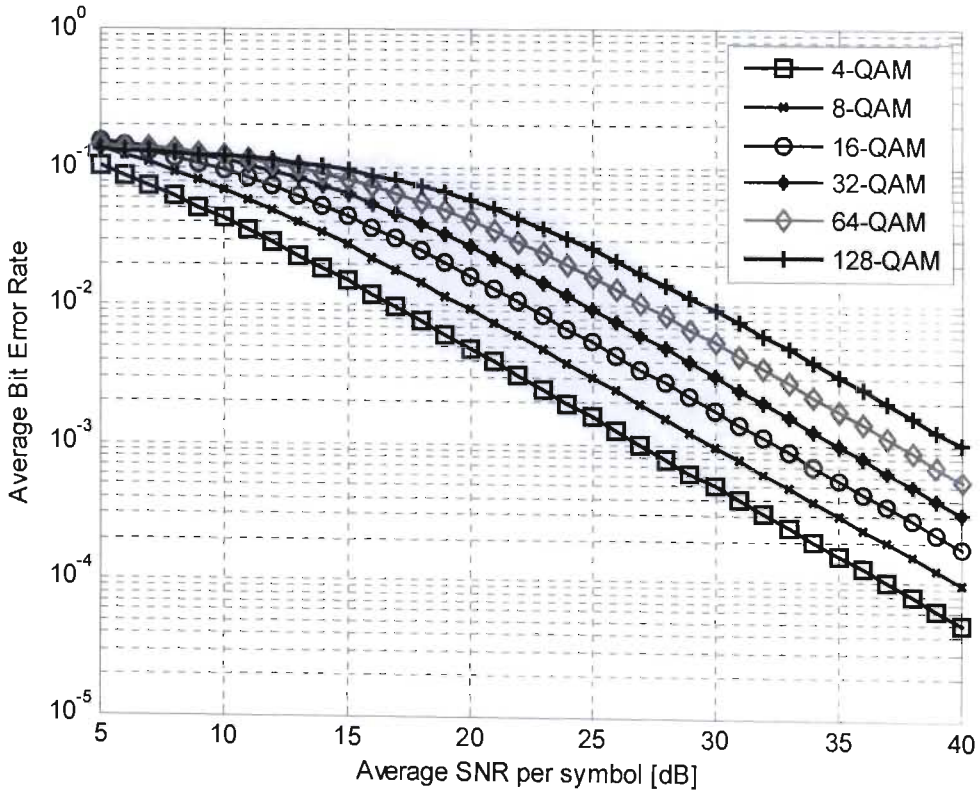

Figure 3-3: Average BER for M-QAM modulation over $m = 1$ Nakagami-m fading

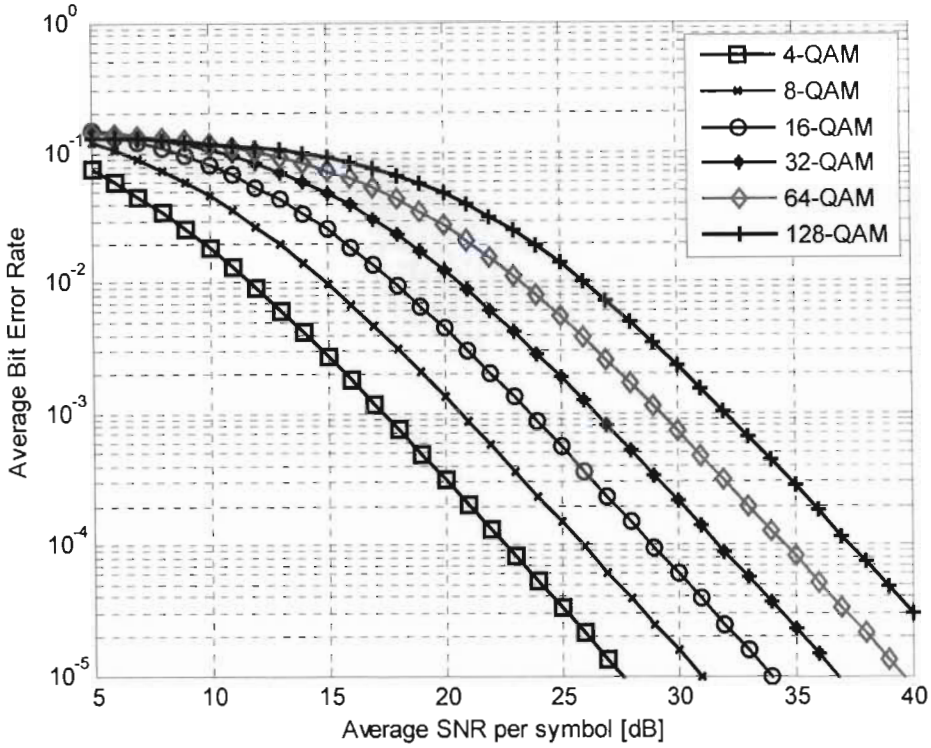

Figure 3-4: Average BER for M-QAM modulation over $m = 2$ Nakagami-m fading

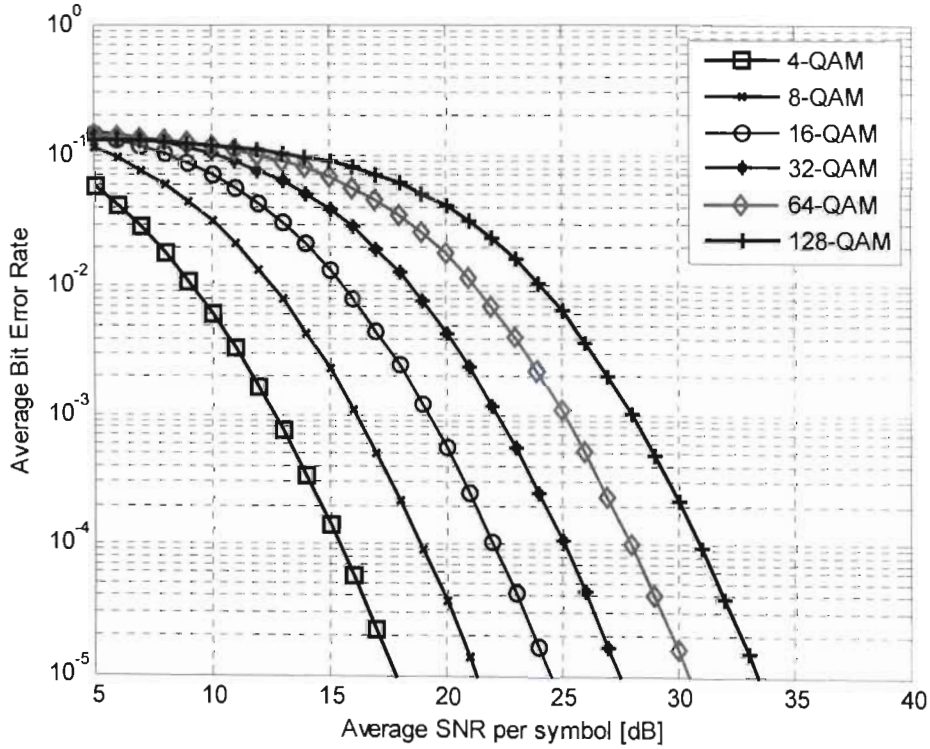

Figure 3-5: Average BER for M-QAM modulation over $m = 5$ Nakagami-m fading

Table 3-1: Boundary points for adaptive M-QAM modulation over $m = 1, 2\ and\ 5$ Nakagami-m fading channels for $BER_0 = 1 \times 10^{-3}$

Mode (n)	2	3	4	5	6	7
	$m = 1$					
M	4QAM	8QAM	16QAM	32QAM	64QAM	128QAM
SNR(dB)	26.96	30.67	32.49	35.02	37.52	40.05
	$m = 2$					
M	4QAM	8QAM	16QAM	32QAM	64QAM	128QAM
SNR(dB)	17.40	21.50	23.67	26.50	29.29	32.06
	$m = 5$					
M	4QAM	8QAM	16QAM	32QAM	64QAM	128QAM
SNR(dB)	12.64	16.93	19.25	22.23	25.14	28.03

Finally simulation results are presented to demonstrate the improved accuracy of the adaptive M-QAM modulation scheme over a Nakagami-m fading channel. The BER performance of the system shows that the proposed scheme meets its BER target of 1×10^{-3}. Figure 3-6, 3-7 and 3-8 shows that there is a much tighter fit between the analytical expression and simulation curves for Nakagami-m, $m = 1$, than those of previous studies referenced. Figure 3-6, 3-7 and 3-8 also demonstrate that the system BER_0 target is met throughout the operable SNR range for $m = 1, 2\ and\ 5$. Unlike the results presented in [24, Fig 7], Figure 3-6 shows that there is no transmission below the SNR point γ_2, which corresponds to the instantaneous SNR boundary for 4-QAM. For a Nakagami-m fading channel, transmitting below this SNR point using 4-QAM will result in an average BER value higher than the BER_0 target. The graph also shows that the average BER performance higher than γ_7 is dominated by the highest modulation mode (128-QAM) of the adaptive scheme.

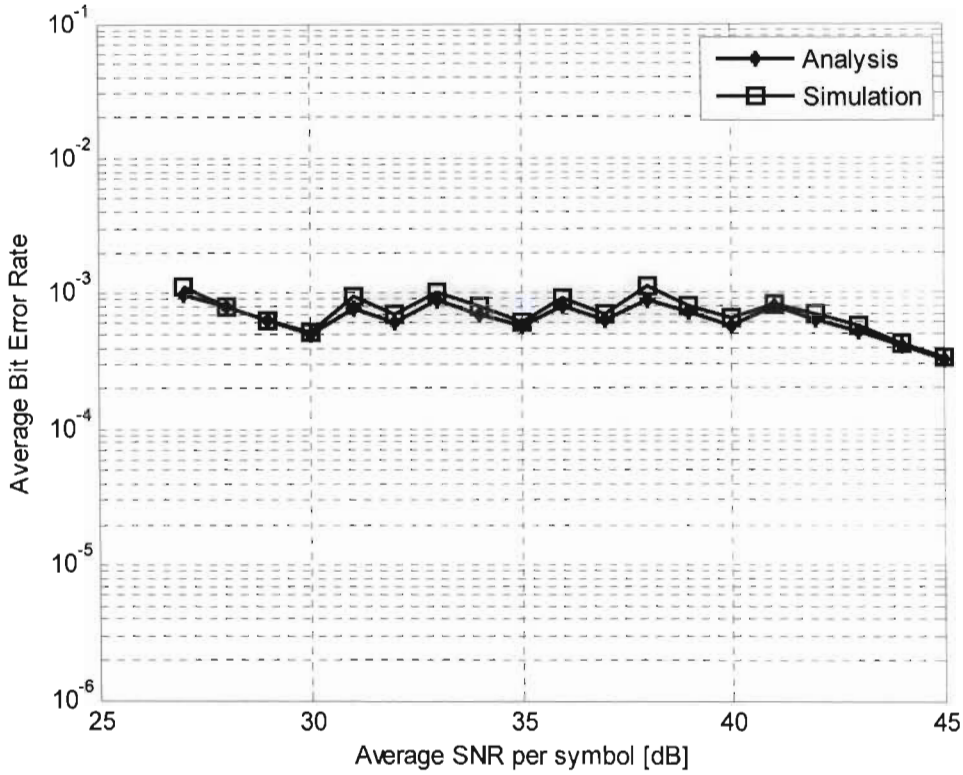

Figure 3-6: Average BER of the adaptive M-QAM over an $m = 1$ Nakagami-m fading

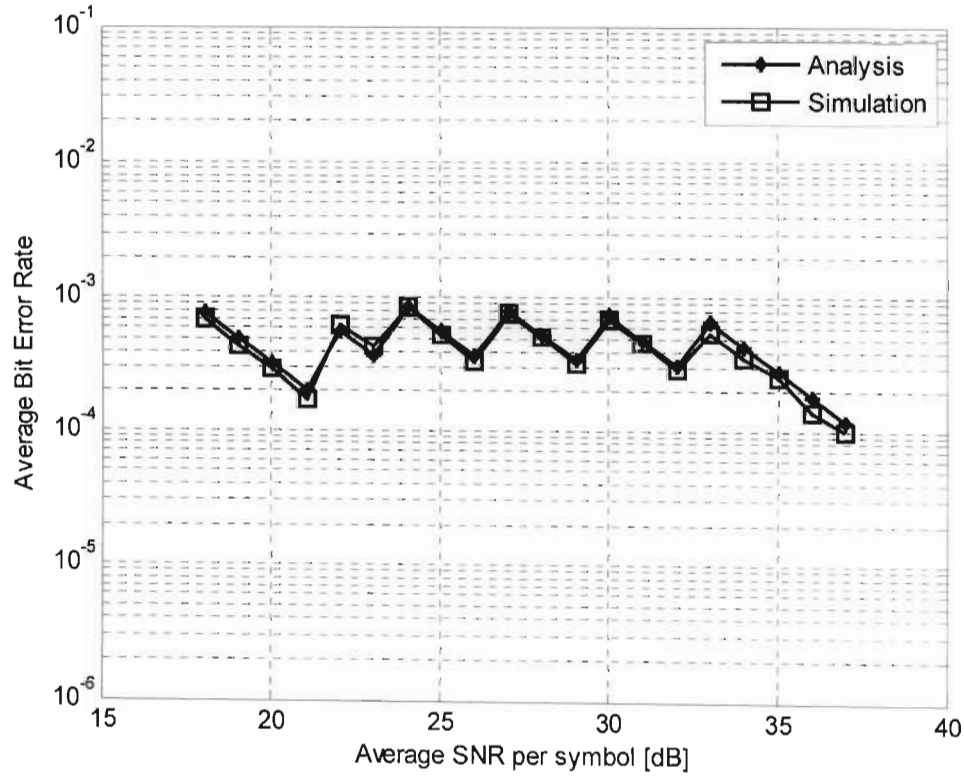

Figure 3-7: Average BER of the adaptive M-QAM over an $m = 2$ Nakagami-m fading

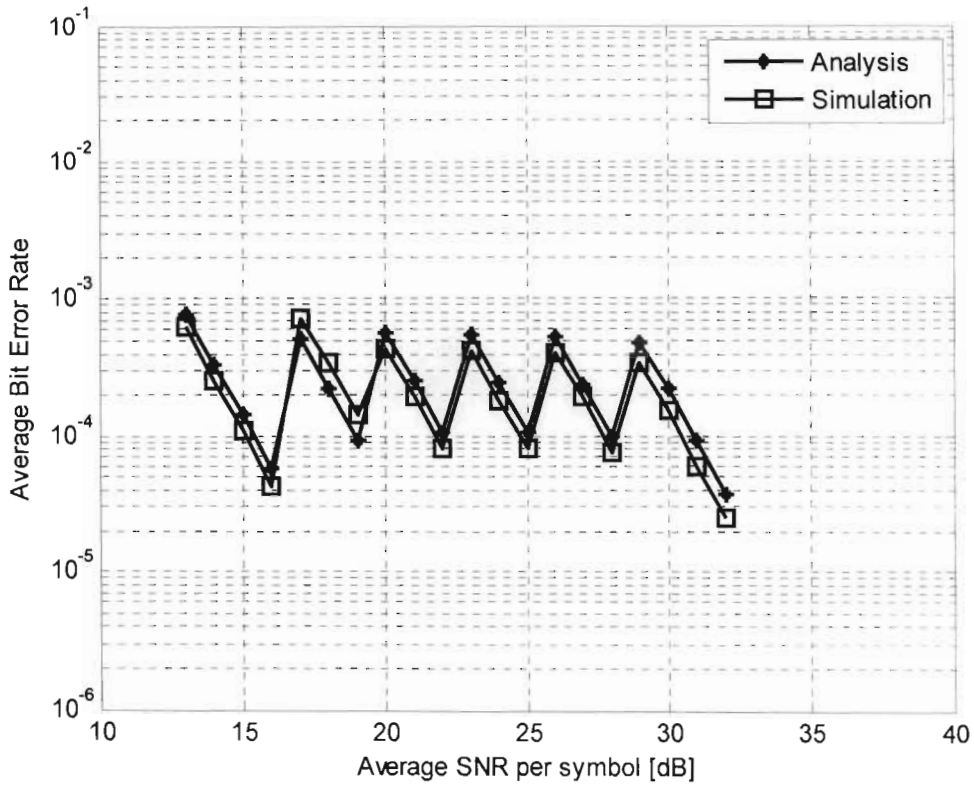

Figure 3-8: Average BER of the adaptive M-QAM over an $m = 5$ Nakagami-m fading

3.5 Conclusion

To improve the accuracy of the channel adaptive M-QAM system BER performance, the average BER over a Nakagami-m fading channel was re-derived using two alternative approximate BER expressions for M-QAM in AWGN. The threshold values for the adaptive M-QAM system were then determined using one of the average BER expressions. Finally simulation results were used to verify the accuracy of the new threshold points and the new average BER expression over the Nakagami-m fading channel.

Chapter 4

Cross-layer design for QoS provisioning

4.1 Introduction

Cross-layer design has been proposed as a methodology to extend the paradigm of single, independent layer optimization to adaptation and optimization across multiple interdependent layers. Recently many cross-layer adaptation mechanisms have been proposed which attempt to solve the QoS provisioning problem. However, most of these schemes [2-18] only focus on interactions between lower (physical and data link) layers and ignore the possibility of sharing information with, and thus combining, higher layers in the optimization process. The drawback to this are the introduction of functional and efficiency limitations, which could be eliminated if higher layers were included. In this chapter one such limitation is highlighted, namely the inability to insert more than one class of traffic in a physical layer frame and the motivation for overcoming this limitation using cross-layer design is presented.

4.2 Related work

The desired outcome of QoS provisioning schemes for multimedia traffic varies from one scheme to the next and is incorporated into the QoS metric emphasized by a particular scheme. A good review of this discussion is provided in [1] and includes example solutions to the problem. The work in [17, 45-46] considers packet delay violation as the main metric while the work in [47] uses handoff dropping probability and average allocated bandwidth. Other QoS metrics include packet loss rate through buffer overflow [45], throughput and fairness [11, 15]. These are MAC or higher layer based adaptive cross-layer schemes which assume that the physical layer is either error free or adapts to the channel to guarantee a single error target; and is independent of the upper layers in its operation.

QoS provisioning using cross-layer design has been proposed by combining the physical and Data Link layers of the protocol stack [29-30]. In these schemes multiuser scheduling at the MAC layer is used with a channel adaptive AMC module at the physical layer which

guarantees a single error target. The consequence of having a single error target is that each frame can only hold one class of traffic. In the concluding section of their paper [30] the authors note this limitation and suggest that multiple connections allowing heterogeneous traffic may lead to better performance. The work in [44] has a similar objective to the one proposed in this paper, namely to allow the transmission of different classes of traffic in a single unit of transmission, however theirs is a CDMA setting and has a higher degree of freedom during resource allocation, as compared to the schemes in [29-30]. The *effective capacity* model [38] has been employed in cross-Layer resource allocation mechanisms for achieving statistical QoS guarantees in terms of delay violation in the transmission of heterogeneous traffic. This model was used in [44] and more recently in the work in [45]. The works in [17, 46] study the scheduling of heterogeneous traffic over wireless links. The objective of both the schemes is to determine the order in which the packets in the queue should be transmitted, thus allowing for only a single packet to be transmitted in a frame. Furthermore, the high computational cost of both the schemes is a disadvantage. The cross-layer mechanism in [49] exploits coupling between the physical and MAC to achieve multi-user diversity. However, because the scheme does not consider the type of traffic being transmitted, the opportunity for diversity across multiple classes of traffic with different QoS requirements is missed. In this chapter the benefit of exploiting diversity across multiple classes of traffic is discussed.

4.3 System model QoS provisioning cross-layer design

A cross-layer multiuser scheduling scheme with prescribed QoS guarantees in adaptive wireless networks was proposed in [29-30]. In these schemes traffic is classified into types and each type has a certain set of QoS requirements. The cross-layer mechanism, which is a combination of a multiuser scheduler at the medium access control (MAC) sub-layer of the data link layer and the adaptive modulation and coding (AMC) of the physical layer, coordinates the transmission of the different types of traffic while adapting to the channel variation for each user.

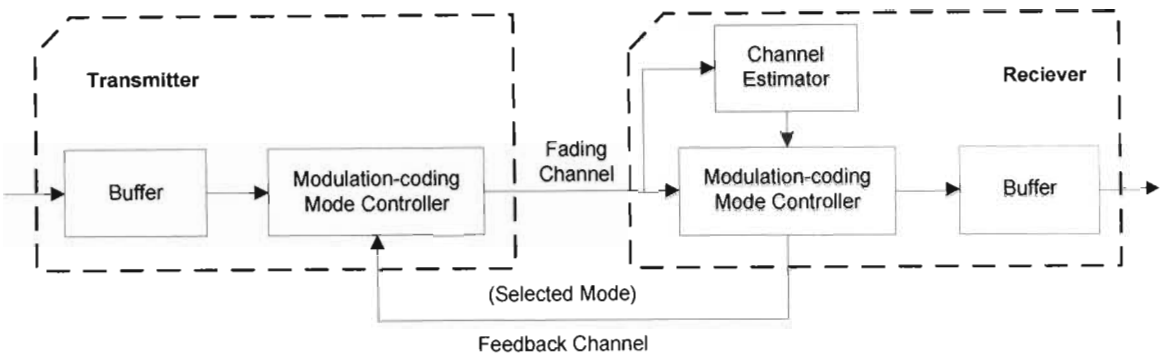

Figure 4-1: Wireless link from the central unit to each user

Figure 4-1 models the proposed system considered in [29]. The link between one of the multiple users or nodes connected to a central unit which could be a base station or a backbone gateway is shown. The transmissions are assumed to be over wireless fading channels using time-division multiplexing/time-division multiple-access (TDM/TDMA).

A finite length buffer is implemented at the central unit for each user and operates in a first-in-first-out (FIFO) mode. The AMC controller follows the buffer (queue) at the central unit (transmitter) and the AMC selector is implemented at each user (receiver). The processing unit at the *data link layer* is a packet consisting of multiple information bits. The processing unit at the *physical layer* is a frame consisting of multiple transmitted symbols. It is assumed that multiple transmission modes are available at each user, with each mode representing a pair of a specific modulation format and a FEC code as in the HIPERLAN/2 and the IEEE 802.11b standards. The modes are designed such that the transmission rate R_n (bits per symbol) is in ascending order with the index n. Thus the rates from modes $n = 1, 2, \ldots, 5$ are $R_n = 0.5, 1.0, 1.5, 3.0, 4.5$ bits/symbol respectively. The details of the transmission modes can be found in [29, Table I]. Based on the channel estimation obtained at the receiver, the AMC selector determines the mode n, which is sent back to the transmitter through an error free feedback channel, for the AMC controller to update the transmission mode. Coherent demodulation and maximum-likelihood (ML) decoding is used at the receiver. The decoded bit streams are mapped to packets which are then transferred to the data link layer at the receiver.

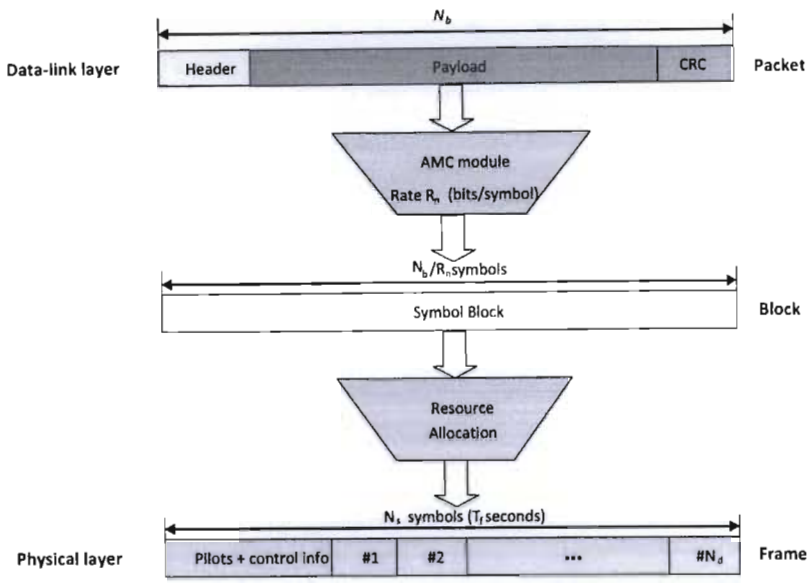

Figure 4-2: Packet structure at each layer

Figure 4-2 shows the packet structure at each layer of the cross-layer scheme [29]. At the data link layer, each packet contains a fixed number of bits (N_b), which includes the packet header; data payload and the cyclic redundancy check (CRC) bits. The packet is then passed to the AMC module which uses mode n of rate R_n to map the bits into a symbol block containing N_b/R_n symbols. At the physical layer, the data is transmitted frame by frame through the fading channel. A block fading channel is assumed in which the channel is frequency flat and remains constant per frame but varies from to frame. Thus the AMC module adjusts its parameters in a frame by frame basis. With TDM, each frame is divided into $N_c + N_d$ time slots, where N_c time slots contain control information and pilots and N_d contains the data. The data slots are scheduled to different users with TDMA dynamically.

The packet error rate (PER) QoS target is guaranteed by the operation of the AMC module at the physical layer [29]. The objective of the module is to maximize the data rate by adjusting transmission parameters to the channel conditions, while maintaining a prescribed packet error rate P_0. Assuming the AMC uses N number of transmission modes, the entire SNR range is partitioned into $N + 1$ non-overlapping consecutive intervals with boundary points denoted as $\{\gamma_n\}_{n=0}^{N+1}$. The mode selector at the receiver selects mode n when $\gamma \in [\gamma_n, \gamma_{n+1})$. The design objective of the AMC is to determine the boundary points $\{\gamma_n\}_{n=0}^{N+1}$ so that the average packet error rate for each mode is exactly P_0. The details the AMC module design can be found in [29] and the references therein.

4.4 Limitation for current system

The limitation of this cross-layer scheme can be found in the method it uses to guarantee the packet error rate (PER) QoS targets for different classes of traffic. Multimedia transmission consists of voice, video and data traffic, and each class of traffic has its own QoS target in terms of packet error rate. Typical PER targets for voice, video and data are $10^{-1}, 10^{-2}$ and 10^{-4} respectively [44]. However, since the AMC module only guarantees a single value for PER in its design, once a target PER P_0 has been chosen for a frame (depending on the QoS requirement of the type of traffic being transmitted), then only that type of traffic can be inserted into the frame. If P_0 is set for voice traffic then, although the AMC will ensure that the PER target for voice will be met, the PER will not be low enough for video or data, if such traffic were to be inserted into the frame. At the other end of the scale, if the PER target is set for data traffic, the AMC system operation will be inefficient in its transmission of voice and video traffic. The functional limitation is shown diagrammatically in Figure 4-3 and Figure 4-4, where the packets in a frame labelled 'V' represents voice packets while 'D' represents data packets. The current system will allow the scheduling of a frame structure as shown in Figure 4-3 but not one that is shown in Figure 4-4.

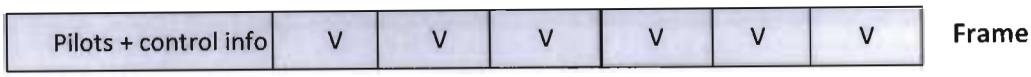

Figure 4-3: Frame structure allowed in the current system

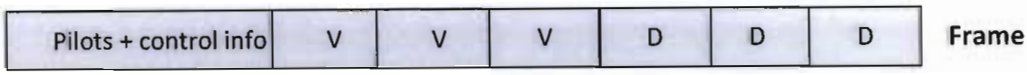

Figure 4-4: Frame structure not allowed in the current system

Echoing the comments made by the authors in [30] it is proposed in this thesis that the efficiency of the resource allocation module of a cross-layer QoS provisioning system would be noticeably higher if heterogeneous traffic could be inserted into a single frame and it had a finer control over the allocation of resources for the different classes of traffic being transmitted. In order to facilitate this functionality, the paradigm of the cross-layer design discussed in this chapter is extended in the next chapter where the AMC and data link module is combined with a channel adaptive coding mechanism at the application layer to guarantee QoS performance in terms of PER for voice, video and data traffic.

4.5 Conclusion

A QoS provisioning cross-layer design has been discussed in this chapter. The system model and operation of the scheme was briefly outlined. More importantly, it was discussed how the scheme's mechanism for guaranteeing packet error rate for different multimedia traffic types has a functional limitation, which if overcome can lead to improvements in terms of resource allocation efficiency. The next chapter discusses a cross-layer mechanism which will overcome the functional limitation discussed in this chapter and facilitate the improvement in terms of efficiency.

Chapter 5

Physical and application layer cross-layer design for multimedia traffic transmission

5.1 Introduction

A physical and data link layer cross-layer mechanism for guaranteeing PER targets in wireless channels was discussed in the last chapter. An analysis of the operation of the cross-layer design showed that it introduces functional limitations in that a physical layer frame can only contain one class of traffic. In this chapter the cross-layer mechanism is extended to include a channel adaptive coding scheme at the application layer which offers adaptive error protection depending on the class of multimedia traffic being transmitted in the frame.

The concept of combining the physical and the application layer for error protection has been applied in the area of video transmission over wireless links [50-51]. The physical layer parameters are adapted to the different channel conditions while an application layer FEC provides an additional error control strategy. The novelty in the use of an application layer FEC for video transmission is that it can offer the flexibility of unequal or selective error protection. A multiple description source encoder splits a video stream into multiple bit streams or descriptions, and each sub-stream has a different priority. The priority is based on the level of fidelity with which each sub-stream describes the original stream. Thus a higher level of FEC protection is then applied to a high priority bit-stream than one with a lower priority.

The system proposed in this chapter applies the unequal error protection concept mentioned above to the three classes of traffic to be transmitted over the wireless link. Data traffic has the highest priority in terms of QoS error protection and receives the highest level of protection while voice traffic, having lowest priority, receives the lowest level of protection, and the level of protection for video traffic is in between the two.

5.2 System model

5.2.1 System description

The system under consideration has multiple users or nodes connected to a central unit which could be a Base Station or a backbone gateway for a WLAN or ad hoc network. Each user/node is connected to the central unit over the wireless channel using time-division multiplexing/time-division multiple-access (TDM/TDMA). Only the downlink is considered in this system, with the assumption that the results for the uplink would not be dissimilar.

The wireless link between two nodes is shown in Figure 5-1.

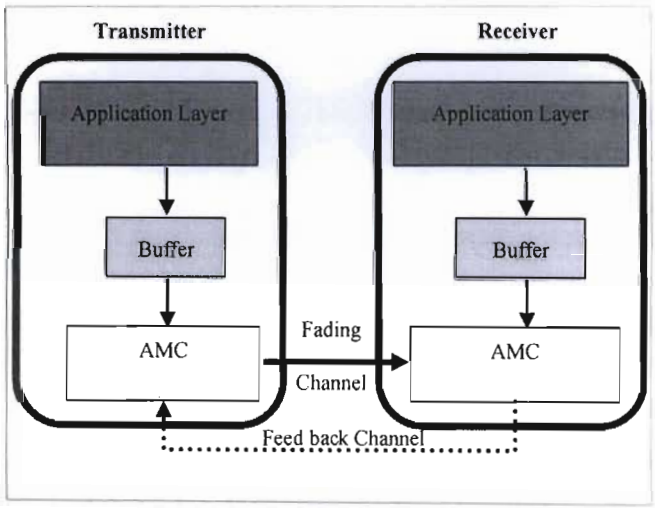

Figure 5-1: Wireless link between communicating nodes

This is a modification of the model used in other AMC schemes, as the ones presented in [29-30]. The main differences between these schemes and the one proposed in this chapter are as follows:

a) The schemes in [29] and [30] only accommodate one class of traffic while the proposed scheme accommodates multiple classes of traffic.

b) The schemes in [29] and [30] use only the physical and data link layer while the proposed cross-layer design adds a third layer, in the form of the application layer, to cater for multiple classes of traffic.

In the proposed scheme, the AMC module at the physical and data link layer provides a certain level of error protection which is the same as in [29-30]. The application layer

module, using an adaptive application layer coder, provides additional error protecting to different classes of traffic by varying its coding parameters; depending on the channel conditions and the class of traffic being transmitted. Thus the three layers combine to guarantee QoS (in terms of error performance) to various classes of traffic. A buffer (queue) is implemented at the central node for each user and operates in a first-in-first-out (FIFO) mode. The AMC module follows and precedes the buffer at the transmitter and receiver respectively. The AMC controller is implemented at the central node (transmitter) and an AMC channel estimator at each user (receiver).

The traffic (voice/video/data) streams are encoded by the coder at the application layer to form code blocks. These code blocks are passed to the data link layer as packets which are then stored in the buffer waiting to be served by the AMC module of the physical layer. After the AMC module processing, the symbols are packaged into a frame which is transmitted over the wireless channel. The AMC module allows each user to have multiple transmission modes, each of which represents a pair of a specific modulation format and an FEC code. Such transmission modes are implemented in systems operating the HIPERLAN/2 and IEEE 802.11a protocol standards. Channel estimation is done at the receiver and the results are fed back to the transmitter. This information is fed to both the AMC controller and the adaptive application layer coder, and they adjust their parameters accordingly. The channel state information (CSI) is used by the AMC controller to determine a modulation-coding pair (or mode) and by the application layer coder to determine a coding rate.

5.2.2 Packet structure at various layers

- ***The application layer***: The voice, video or data packets are encoded into Reed Solomon (RS) code blocks. The encoder takes k data symbols of L bits each and adds parity symbols to make an n symbol code word/block.
- ***The data link layer***: Each packet contains a fixed number of bits (N_b) and this includes the packet header, the payload from the application layer coder and cyclic redundancy check code (CRC) bits. Each packet is mapped to a symbol block containing N_b/R_n symbols where R_n is the rate for mode n.
- ***The physical layer***: Each frame contains a fixed number of symbols (N_s). The symbol rate is fixed and so the frame duration (T_f) remains constant. With TDM, the frame is divided into $N_c + N_d$ time slots, where N_c is the number of time slots with control information and pilots while N_d is the number of time slots that convey the

data being transmitted. Each time slot contains a fixed number of N_b/R_1 symbols [29]. Given a transmission mode n, each time slot will then contain R_n/R_1 packets. For example a time slot will contain $R_n/R_1 = 1$ packet with mode $n = 1$, $R_n/R_1 = 2$ packets with mode $n = 2$ etc.. The data time slots are scheduled to different users using TDMA dynamically. The aim of this work is to allow various class of traffic to be transmitted to one user or many users in the same frame.

The data structures at the interacting layers are shown in Figure 5-2.

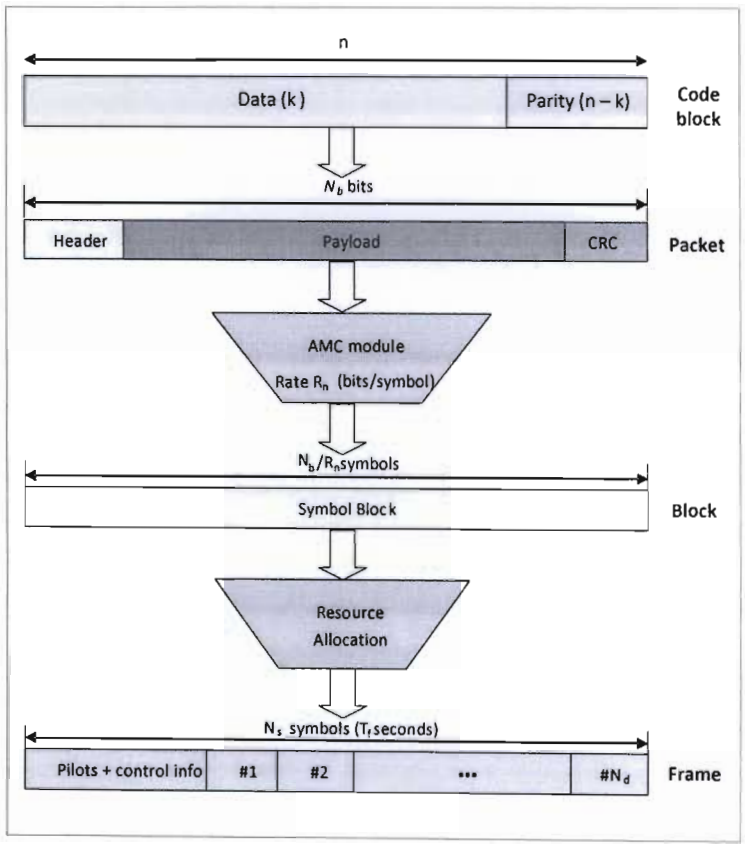

Figure 5-2: Data structures at the interacting layers

5.2.3 Operating assumptions

The channel model assumed for this system is a block fading model where the channel between users is frequency flat and invariant for the duration of one frame, but varies from frame to frame. Such a model is suitable for slowly varying wireless channels [30]. The adaptive schemes at the physical and application layer are then adjusted on a frame-by-frame basis. Perfect CSI is available at the receiver which is derived from training-based channel

estimation. The feedback channel is assumed to be error free and instantaneous, thus the determined SNR value is fed back to the transmitter without error and latency.

5.3 System design

5.3.1 Physical layer

The objective of the adaptive algorithm at the physical layer is to maximize the data rate, while maintaining the required bit error rate (BER) performance at a target value. The transmission modes (no coding is used currently in the system) at the physical layer are arranged such that the rate increases as the mode index n increases. This is shown in Table 5-1.

Table 5-1: Boundary points for adaptive non-coded modulation, given $BER = 1 \times 10^{-3}$

Mode (n)	1	2	3	4	5	6	7
M	BPSK	4QAM	8QAM	16QAM	32QAM	64QAM	128QAM
SNR(dB)	6.79	10.25	13.93	17.24	20.39	23.47	26.52
R_n	1	2	3	4	5	6	7

Let N denote the total number of transmission modes available. Assuming constant power, the received SNR (γ) range is partitioned into $N+1$ non-overlapping consecutive fading intervals with the boundary points denoted as $\{\gamma_n\}_{n=0}^{N+1}$.

Mode n and thus the constellation size M is chosen when: $\gamma \in [\gamma_n, \gamma_{n+1})\ for\ n = 1, 2, \ldots, N$

To avoid deep fades, no payload bits are sent when the SNR (γ) is below a certain threshold (γ_1). Table 5-1 shows the boundary points for the non-coded modulation scheme for a target BER value of 10^{-3} (appropriate for voice traffic) using M-QAM over an AWGN channel. The expressions used to determine the boundary points for the adaptive M-QAM system are derived in [22] as detailed in chapter 2 and are reproduced here as

$$\gamma_1 = [erfc^{-1}(2BER_0)]^2, \text{ for BPSK}, \tag{5.1}$$

$$\gamma_n = \frac{2}{3}K_0(2^n - 1); \quad n = 2, 3, \ldots, N; \text{ for M-QAM}, \tag{5.2}$$

$$\gamma_{N+1} = +\infty, \tag{5.3}$$

where $erfc^{-1}(.)$ denotes the inverse complementary error function and $K_0 = -ln(5BER_0)$. All of the thresholds or boundary points (except for γ_1) are calculated using (5.2), which is the inverse of the following BER approximation [22, eq 28]

$$P_b(\gamma) \cong 0.2exp\left(\frac{-3\gamma}{2(M-1)}\right) \tag{5.4}$$

As discussed in chapter 2, the authors in [22] motivate the use of the approximation by the fact that both (5.4) and its inverse (5.2) are very simple functions which lead to closed-form analytical expressions and that further insights are unattainable with more complicated BER expressions. However, (5.4) is an upper-bound for the BER only for $M \geq 4$ and thus γ_1 is chosen according to the exact BER performance of BPSK. The inverse of (5.1) used to determine the BER performance of BPSK is given by:

$$BER_{BPSK}(\gamma) = Q\left(\sqrt{2\gamma}\right) \tag{5.5}$$

When the switching thresholds are chosen according to the boundaries using (5.1) and (5.2), the physical layer will ensure a BER performance that is below the target BER.

5.3.2 Application layer

The BER performance target chosen at the physical layer was 10^{-3}. This error target, although sufficient for voice applications, is not low enough for more demanding applications such as video and data. In order to accommodate these types of traffic in the system, additional error protection is required. The variable error protection is achieved in this cross-layer design (CLD) system using Reed-Solomon (RS) codes at the application layer.

The metric for error rate performance in most applications, such as video, is the frame error rate. The analytical expression for frame error rate for general RS codes is as follows.

The frame error probability (P_{fe}) can be expressed as shown in (5.6):

$$P_{fe} = \sum_{k=t+1}^{N} \binom{N}{k} (1-P_s)^{N-k} P_s^k , \tag{5.6}$$

where N is the number of code symbols per frame, t the number of code symbols that the code can correct, P_s the symbol error probability and k the number of data symbols.

Then, P_s, can be expressed as

$$P_s = 1 - (1 - P_b)^L , \tag{5.7}$$

where P_b is the bit error probability (calculated using (5.4)) and L the number of bits per code symbol.

The frame error rate was evaluated for RS(127, k) and RS(63, k) codes with error correcting capabilities of t = 1, 2, 3 and 4 over an AWGN channel within the range for each mode of the AMC module. The frame error rate performance for RS(127, k) and RS(63, k) can be seen in Figure 5-3 and 5-4, respectively.

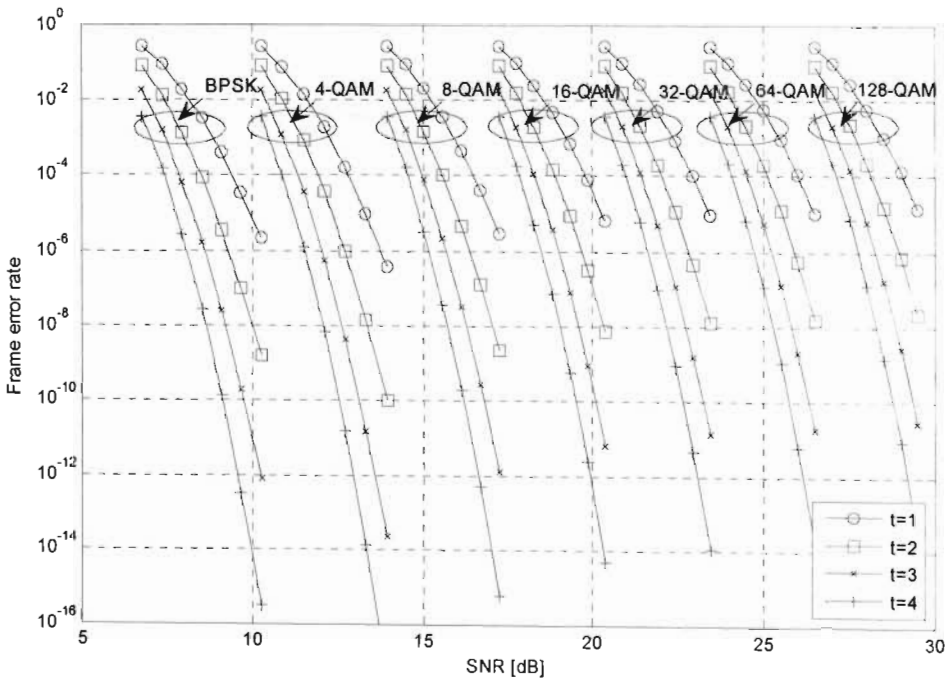

Figure 5-3: Frame error rate performance for RS(127,k)

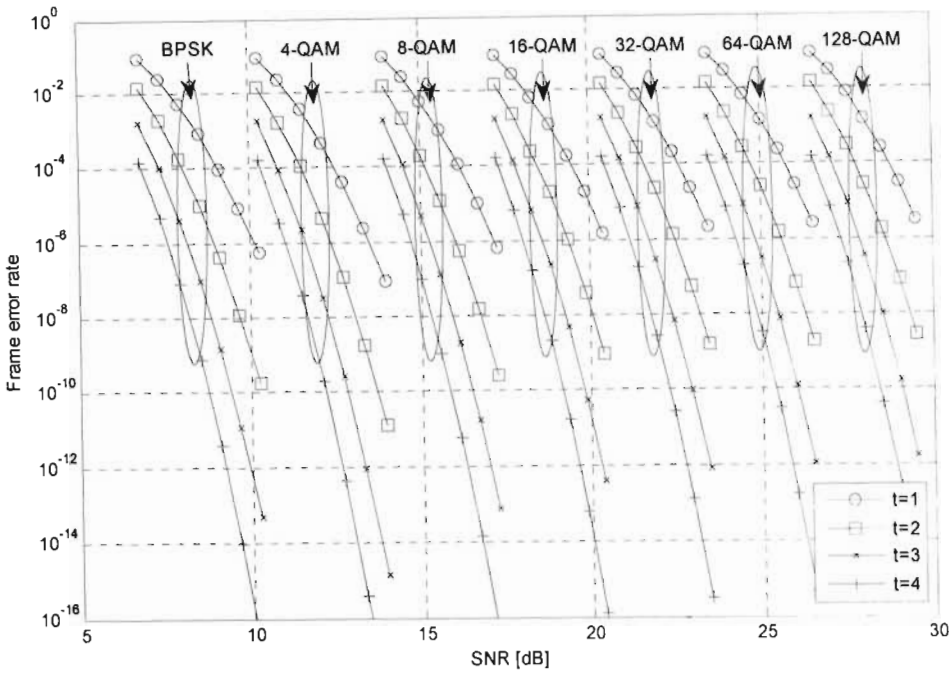

Figure 5-4: Frame error rate performance for RS(63,k)

The k value, i.e., the level of protection for each class of traffic, depends on the P_{fe} target and the SNR value fed back from the receiver. The boundaries in the SNR range for each k value was determined by setting P_{fe} targets for each class of traffic. The target P_{fe} for voice, video and data was 10^{-1}, 10^{-2} and 10^{-4} respectively. These target values are similar to those used in the performance evaluation of the scheme in [44], but in this case they are used to design the SNR thresholds for the level of protection at the application layer for each class of traffic. The k values and the respective SNR threshold values guaranteeing the P_{fe} target for each traffic class was determined numerically using expressions (5.6) and (5.7).

The overall operation of the cross-layer design is as follows. There is a separate queue at the central unit for each active traffic session with the users with which it is communicating. Before the transmission of a frame, once it obtains the CSI information (i.e. the channel gain) from the receiver, the AMC module uses the value to select the appropriate mode, ensuring that BER rate is no higher than 10^{-3}. The channel gain information is also passed to the application layer coder and it uses the value to determine k in a RS (n, k) code for each class of traffic being transmitted. Thus a different k value will be selected for voice, video and data traffic, and this value will be used by the RS encoder. The output code blocks, which could contain any of the three classes of traffic, are passed to the AMC module as packets. The AMC module then produces symbol blocks using the selected mode and they

are inserted into the time-slots of the frame to be transmitted. The process is reversed at the receiver. The AMC module processes the received frame and produces packets which could be either a voice, video or data packet. At the application layer, the packet header is examined to find out the k value that was used in the encoding process and this is then passed to the RS decoder. The decoder then decodes the packet and passes it to the appropriate application.

The two interacting layers (application and physical) are combined to guarantee that the target error rate for each class of traffic being transmitted is achieved. However, they operate quite independent of each other since the physical layer makes no distinction between the packets that it receives from the application layer. The packets are inserted into the frame which is modulated by a single AMC mode. Thereafter, the application layer encoder, given the channel gain, selects the k value depending on the class of traffic being transmitted and uses this to encode the packets. Due to this independence, a frame can contain a mix of voice, video and data traffic. This is the ideal form of cross-layer design in which inter-layer coupling is used to achieve a design objective without compromising the structure of the layers.

5.4 System performance

The first task in the system performance analysis was to determine the theoretical performance of the system using the threshold boundary points and analytical expressions for both the AMC module at the physical layer and the variable error protection system at the application layer. The number of bits for each RS code symbol (L) used was 8 bits. Shortened $(255, k)$ RS codes were employed with a codeword length (N) of 127 for voice traffic and 63 for video and data traffic. The performance of the three classes of traffic was determined separately using (5.4) – (5.7), and can be seen in Figure 5-5, 5-6 and 5-7 for voice, video and data respectively.

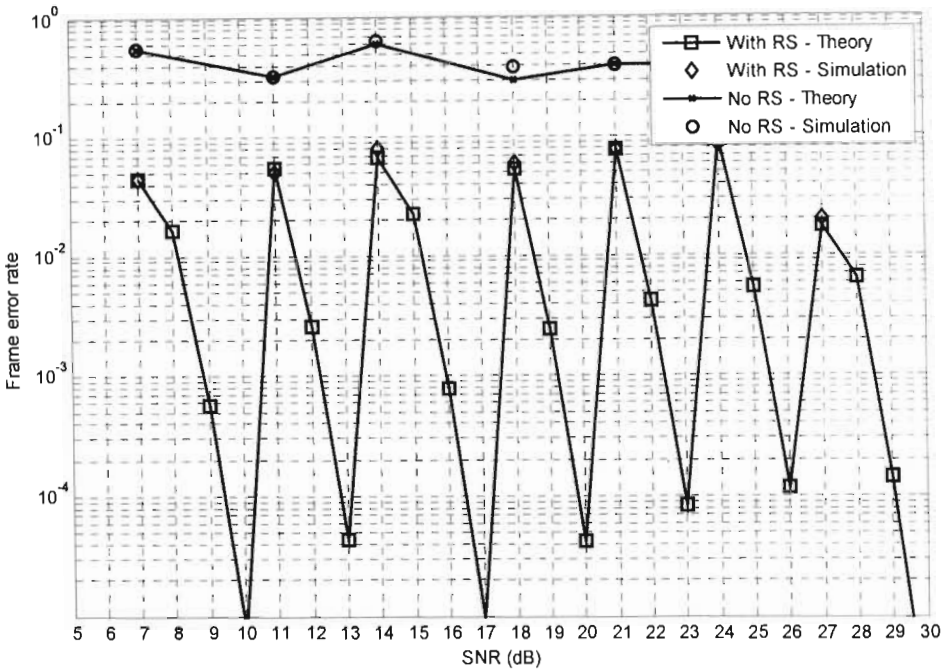

Figure 5-5: Frame error rate performance for voice traffic

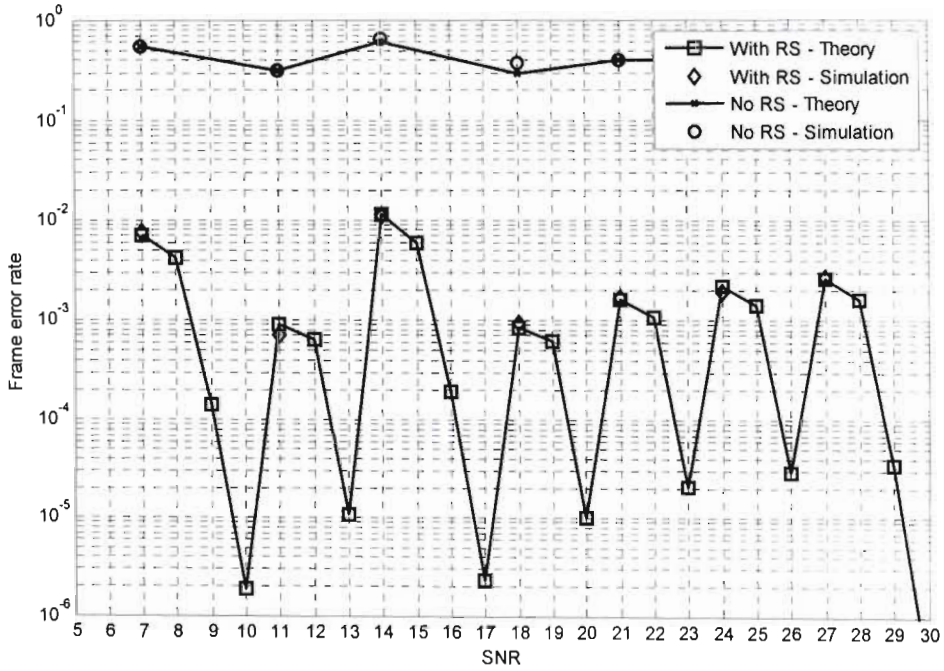

Figure 5-6: Frame error rate performance for video traffic

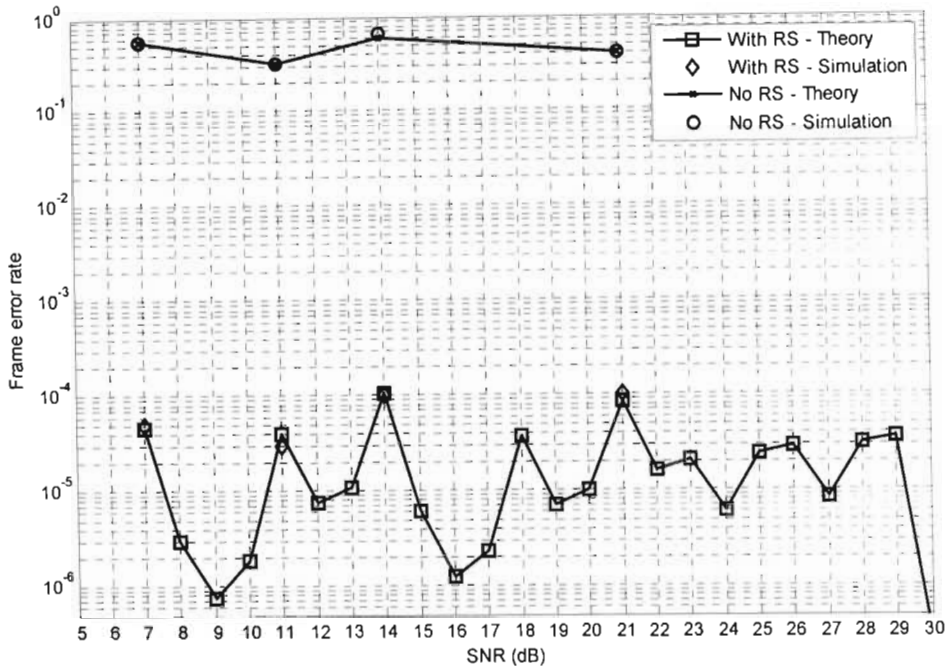

Figure 5-7: Frame error rate performance for data traffic

The system was then simulated at certain SNR points over an AWGN. The message or packet length was NxL and was modulated at the physical layer by the schemes shown in Table 1. Initially the results of the simulations showed noticeable difference from the values expected from the theoretical evaluations for modes with $M_n \geq 4$. This was due to the analytical expression (5.4) which, as discussed in chapter 2, is only an approximation for modulations with $M_n \geq 4$. Due to the sensitivity of the BER performance on the frame error rate results, this difference resulted in the divergence from the theoretical result at the application layer. A compensation factor was introduced that shifted the curves at the physical layer to match the result of the analytical approximation with that derived from the simulation. The boundary points were adjusted accordingly. This resulted in a much tighter fit of the simulation and theoretical results of the overall system, as can be seen in Figure 5-5, 5-6 and 5-7. The objective of these experiments was to prove that the design decisions made in the formulation of the scheme were valid for the purposes of meeting the targets of the cross-layer design. It was also important to prove that an implementation of the physical and application layer cross-layer design would produce the same results as that expected from theory. Thus the simulations were conducted to verify the analytical results.

The graphs in Figure 5-5 to 5-7 show that the performance of the adaptive application and physical layer cross-layer design system meets the target for all three classes of traffic across

the channel SNR range. The frame error rate goes no higher than 10^{-1}, 10^{-2} and 10^{-4} voice, video and data respectively. Thus, having met this objective, the system will allow for the insertion of any of the three classes of traffic, in any combination, in a single physical layer frame without the danger of not meeting frame error rate QoS targets, thus fulfilling the purpose of the proposed cross-layer design system. The overall system benefits include the increased efficiency of the resource allocation mechanism which will now have a fine grain control of the available system resources (timeslots) when scheduling the three classes of traffic.

Figures 5-5 to 5-7 also show the effect of removing the adaptive application layer coder from the system which results in the P_{fe} for each class of traffic being much higher than the set target. This shows the ineffectiveness of only using the adaptive physical layer mechanism in meeting the error rate QoS targets.

5.5 Conclusion

In this chapter a physical and application layer cross-layer mechanism was proposed which will facilitate dynamic resource allocation where more than one or all three classes of traffic considered can be transmitted simultaneously in one frame. The system was designed with the assumption that a block fading channel can be modelled using an AWGN channel and simulation results were used to verify the expected results from the analytical design of the system in such a channel model.

Chapter 6

Cross-layer design for multimedia traffic transmission in a fading channel

6.1 Introduction

It was shown in chapter 2 that the approximation BER expression for M-QAM in AWGN (2.1) that is commonly used to design channel adaptive physical layer systems results in inaccuracies when used in a fading channel. This expression was also used in the last chapter for the design of the AMC module of the physical and application layer cross-layer design with the assumption that slowly varying block fading channels can be modelled as AWGN channels. The system analytical expression, verified by simulations, showed that the simple approximation BER expression is useful in the design of the system for AWGN. However, in this chapter, the more accurate method derived in chapter 3 to calculate the system BER for M-QAM in fading channels will be used to determine the adaptive M-QAM threshold points and physical layer performance for the cross-layer design mechanism.

6.2 System design

The system model, the packet structure, the operating assumptions and the functionality of the cross-layer mechanism is as mentioned in section 5.2. The changes are made to the system design which are as follows.

6.2.1 Physical layer

Assuming there are N transmission modes available, the SNR range is partitioned into $N + 1$ fading intervals. The system is modified in that in that BPSK is no longer used. Thus the index for the threshold boundaries $\{\gamma_n\}_{n=2}^{N}$ now begins at 2 and γ_1 (as opposed to γ_0) is set to 0. The outage region is modified to $\gamma_1 \leq \gamma < \gamma_2$.

The system design in this chapter is for a $m = 2$ Nakagami-m fading channel, however the same procedure can be used for other Nakagami-m channels. Table 6-1 shows the boundary

points for the adaptive M-QAM for the $m = 2$ Nakagami-m channel for QoS BER target (BER_0) of 1×10^{-3}.

Table 6-1: Boundary points for adaptive M-QAM modulation over the $m = 2$ Nakagami-m fading channel for $BER_0 = 1 \times 10^{-3}$

Mode (n)	2	3	4	5	6	7
M	4QAM	8QAM	16QAM	32QAM	64QAM	128QAM
SNR(dB)	17.40	21.50	23.67	26.50	29.29	32.06

As shown in section 3.4 of this thesis, the values for the boundary points were determined numerically using the approximation for the average BER of M-QAM in a Nakagami-m fading channel and is given by

$$P_b(M,\bar{\gamma}) = \frac{a}{p \times k}\left\{\frac{1}{2}\left(\frac{2m}{2m + b\bar{\gamma}}\right)^m - \frac{a}{2}\left(\frac{m}{m + b\bar{\gamma}}\right)^m + (1-a)\sum_{i=1}^{p-1}\left(\frac{mS_i}{mS_i + b\bar{\gamma}}\right)^m + \sum_{i=1}^{2p-1}\left(\frac{mS_i}{mS_i + b\bar{\gamma}}\right)^m\right\}, \quad (6.1)$$

where, $a = \left(1 - \frac{1}{\sqrt{M}}\right)$; $b = \frac{3}{(M-1)}$; $S_i = 2sin^2\left(\frac{i\pi}{4p}\right)$; $\gamma = \frac{E_s}{N_0}$; $\bar{\gamma} = E[\gamma] = \Omega\frac{E_s}{N_0}$; k is the number of bits per symbol, p is the number of summations, m is the Nakagami fading parameter and M represents the M-QAM modulation.

When the adaptive M-QAM switching thresholds are chosen according to the boundaries shown in Table 6-1, the physical layer will ensure a BER performance that is below the target BER.

6.2.2 Application layer

As mentioned in section 5.3.2, the BER target (BER_0) of 1×10^{-3} would only be sufficiently low for voice traffic and the adaptive system would not be able to insert video or data traffic in the same physical layer frame. In order to accommodate these types of traffic simultaneously, additional error protection is required and this is achieved by the user of adaptive RS coding at the application layer.

In order to determine the threshold boundary points for the adaptive RS coding scheme, the frame error rate was evaluated for RS(127, k) and RS(63, k) codes with error correcting capabilities of t = 1, 2, 3 and 4 over the $m = 2$ Nakagami-m fading channel. The expression used is given by

$$P_{fe} = \sum_{k=t+1}^{N} \binom{N}{k} (1 - P_s)^{N-k} P_s^k , \tag{6.2}$$

where N is the number of code symbols per frame, t the number of code symbols that the code can correct, P_s the symbol error probability and k the number of data symbols.

Then, P_s, is given by

$$P_s = 1 - (1 - P_b)^L , \tag{6.3}$$

where P_b is the bit error probability (calculated using the approximate average BER expression (6.1), which is different to the one used in Chapter 5) and L the number of bits per code symbol. The frame error rate performance can be seen in Figure 6-1 and 6-2.

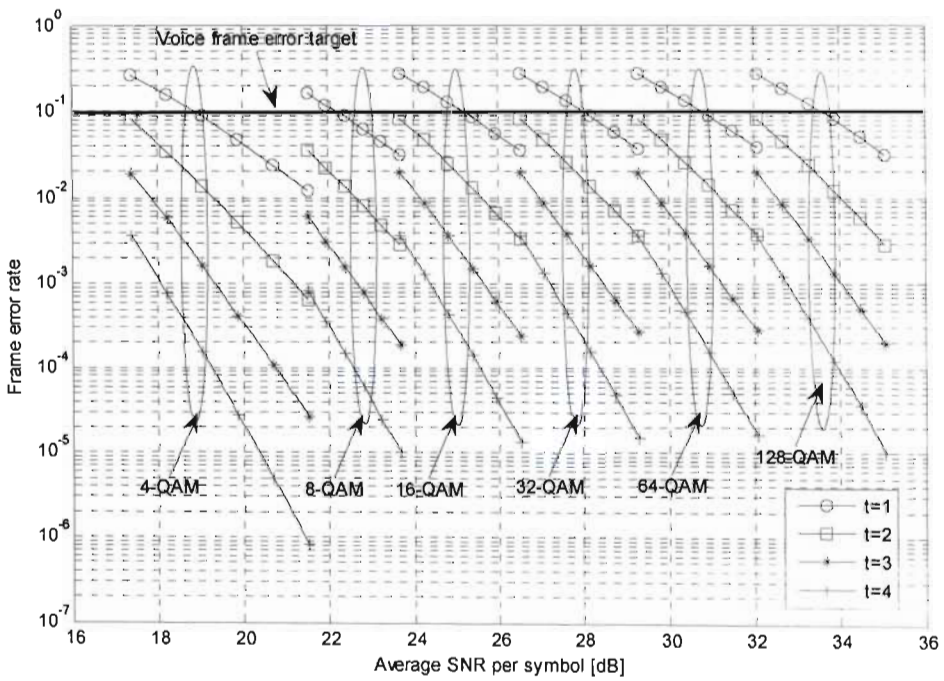

Figure 6-1: Frame error rate performance for RS(127,k)

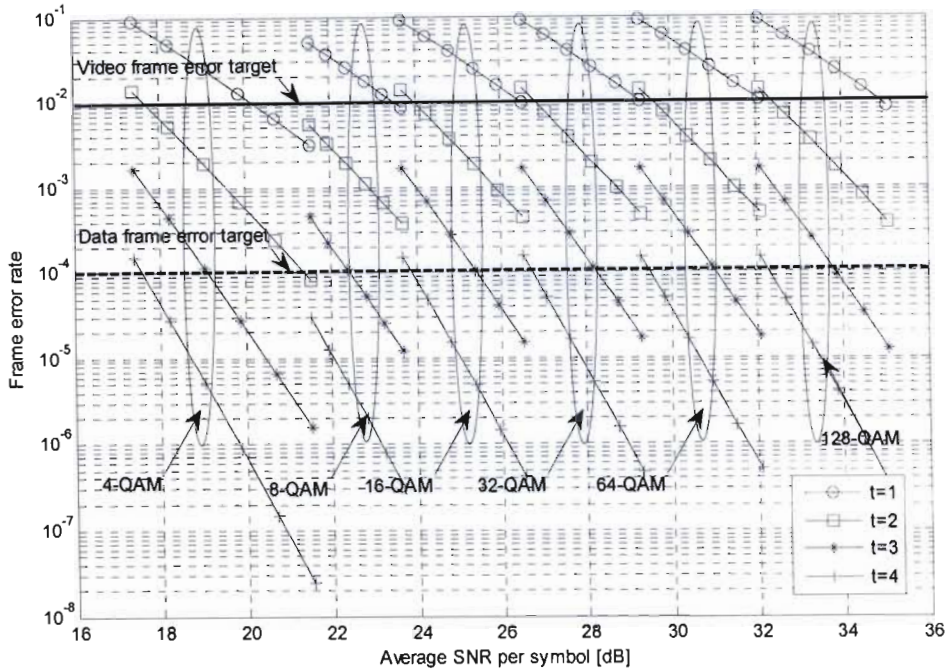

Figure 6-2: Frame error rate performance for RS(63,k)

Using the process discussed in section 5.3.2, the boundaries in the SNR range for each k value (depending on the level of protection for each class of traffic) was determined by setting P_{fe} targets for each class of traffic. The target P_{fe} for voice, video and data was 10^{-1}, 10^{-2} and 10^{-4} respectively. Diagrammatically the target error rate for voice traffic is shown in Figure 6-1, and for video and data it is shown in Figure 6-2 using a solid and a dashed line respectively. The boundary point for a k value for each class of traffic is calculated numerically using (6.2) at the point in the graph where the corresponding t value curve crosses the P_{fe} target line for that class of traffic. The boundary points for the adaptive M-QAM at the physical layer and adaptive RS coder at the application layer application layer are shown for voice, video and data traffic are shown in Table 6-2, 6-3 and 6-4 respectively. The calculation of these boundaries completes the design of the physical and application layer cross-layer mechanism in a $m = 2$ Nakagami-m fading channel. As stated previously, the same process would have to be followed for other Nakagami-m fading channels.

Table 6-2: Boundary points for voice traffic transmission

Voice (P_{fe} target = 10E-1)			
	Left boundary (dB)	Right boundary (dB)	Transmission
	0	17.40	No transmission
Phys. Layer			4QAM
App. Layer	17.40	18.86	N = 127, k = 123
	18.86	21.50	N = 127, k = 125
Phys. Layer			8QAM
App. Layer	21.50	22.18	N = 127, k = 123
	22.18	23.67	N = 127, k = 125
Phys. Layer			16QAM
App. Layer	23.67	25.16	N = 127, k = 123
	25.16	26.50	N = 127, k = 125
Phys. Layer			32QAM
App. Layer	26.50	28.00	N = 127, k = 123
	28.00	29.29	N = 127, k = 125
Phys. Layer			64QAM
App. Layer	29.29	30.79	N = 127, k = 123
	30.79	32.06	N = 127, k = 125
Phys. Layer			128QAM
App. Layer	32.06	33.56	N = 127, k = 123
	33.56	∞	N = 127, k = 125

Table 6-3: Boundary points for video traffic transmission

Video (P_{fe} target = 10E-2)			
	Left boundary (dB)	Right boundary (dB)	Transmission
	0	17.40	No transmission
Phys. Layer			4QAM
App. Layer	17.68	21.15	N = 63, k = 59
	21.15	21.50	N = 63, k = 61
Phys. Layer			8QAM
App. Layer	21.50	23.67	N = 63, k = 59
Phys. Layer			16QAM
AL	23.97	26.50	N = 63, k = 59
Phys. Layer			32QAM
App. Layer	26.80	29.29	N = 63, k = 59
Phys. Layer			64QAM
App. Layer	29.59	32.06	N = 63, k = 59
Phys. Layer			128QAM
App. Layer	32.36	34.88	N = 63, k = 59
	34.88	∞	N = 63, k = 61

Table 6-4: Boundary points for data traffic transmission

Data (P_{fe} target = 10E-4)			
	Left boundary (dB)	Right boundary (dB)	Transmission
	0	17.40	No transmission
Phys. Layer			4QAM
App. Layer	17.60	19.11	N = 63, k = 55
	19.11	21.50	N = 63, k = 59
Phys. Layer			8QAM
App. Layer	21.50	22.43	N = 63, k = 55
	22.43	23.67	N = 63, k = 59
Phys. Layer			16QAM
App. Layer	23.89	25.1	N = 63, k = 55
	25.1	26.5	N = 63, k = 59
Phys. Layer			32QAM
App. Layer	26.72	28.25	N = 63, k = 55
	28.25	29.29	N = 63, k = 59
Phys. Layer			64QAM
App. Layer	29.51	31.04	N = 63, k = 55
	31.04	32.06	N = 63, k = 59
Phys. Layer			128QAM
App. Layer	32.28	33.82	N = 63, k = 55
	33.82	∞	N = 63, k = 59

6.3 System performance

The performance analysis of the cross-layer scheme in a fading channel is presented in this section. The expected theoretical performance of the system in the $m = 2$ Nakagami-m fading channel using the threshold boundary points for both the physical and application layer for the three classes of traffic were determined separately using expressions (6.1) – (6.3) and are shown in Figure 6-3, Figure 6-4 and Figure 6-5 for voice, video and data respectively. The number of bits for each RS code symbol (L) used was 8 bits and shortened ($255,k$) RS codes were used with a code length (N) for voice traffic and 63 for video and data traffic.

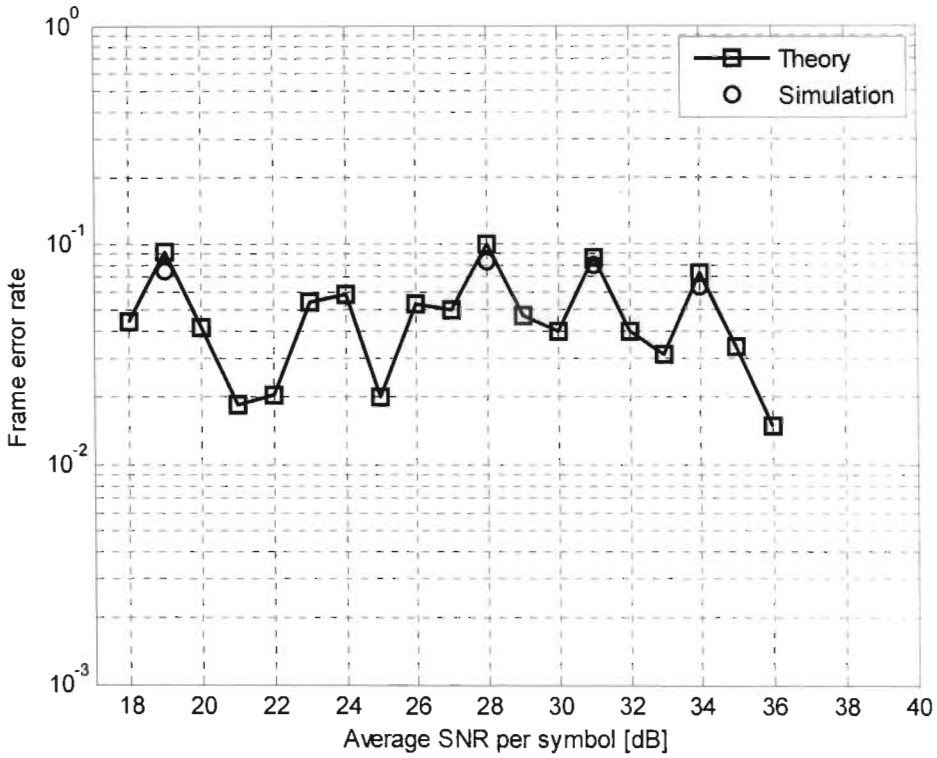

Figure 6-3: Frame error rate performance for voice traffic in $m = 2$ Nakagami-m fading

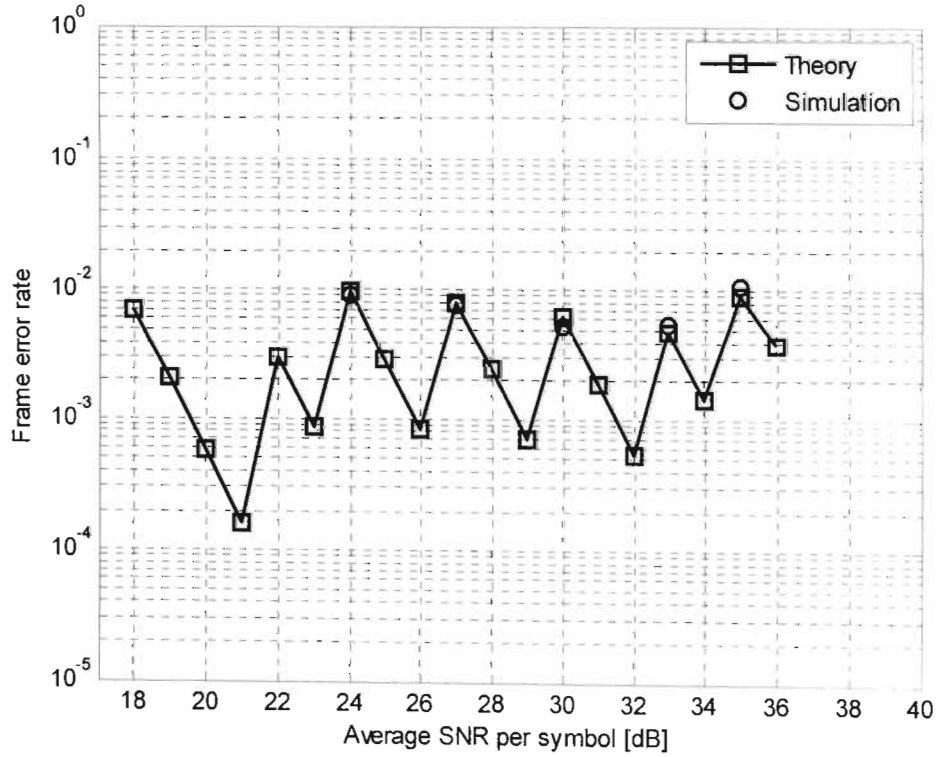

Figure 6-4: Frame error rate performance for video traffic in $m = 2$ Nakagami-m fading

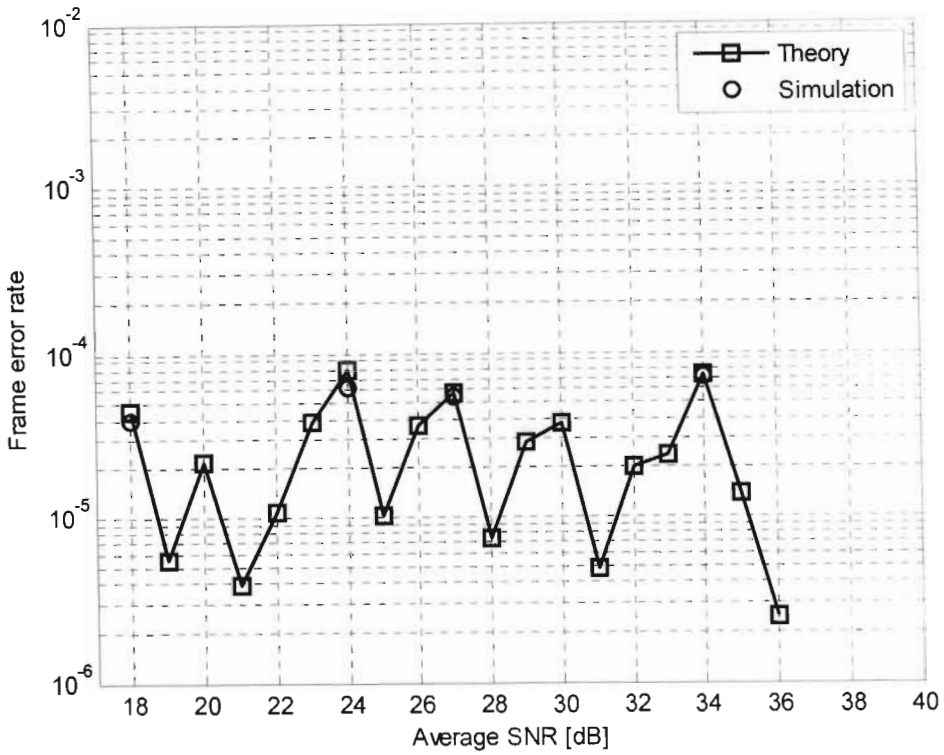

Figure 6-5: Frame error rate performance for data traffic in $m = 2$ Nakagami-m fading

The cross-layer design was then simulated at certain SNR points over a $m = 2$ Nakagami-m fading channel using the simulation method discussed in chapter 3. A slowly varying block fading channel was used. As in chapter 5 this was done to prove that the results of the system implementation in a simulation environment would match the expected theoretical results. The graphs in Figure 6-3, Figure 6-4 and Figure 6-5 show that the simulation results verify the analytical results.

The results in Figure 6-3, Figure 6-4 and Figure 6-5 show that the performance of the adaptive physical and application layer cross-layer mechanism meets the target for all three classes of traffic across the system SNR range in a $m = 2$ Nakagami-m fading channel. A similar conclusion can be made regarding the system in other Nakagami-m fading channels. Thus the channel adaptive cross-layer design meets its objective of allowing for the insertion of multiple classes of traffic in a single physical layer frame while operating in a fading channel while guaranteeing the error rate QoS target for each class of traffic.

The link spectral efficiency performance of the cross-layer system was analysed for a $m = 2$ Nakagami-m fading channel and is presented next. The average link spectral efficiency of the physical layer of the system is determined first using (6.4) [22].

$$\frac{< R >}{W} = \sum_{n=1}^{N} n \times a_n \tag{6.4}$$

where the average link spectral efficiency $< R >/W$ is the rate per unit bandwidth (in units of bits/sec/Hz) of the adaptive M-QAM system over the $m = 2$ Nakagami-m fading channel is the summation of the date rates for each mode n ($n = log_2(M)$) associated with the $N + 1$ regions (N is the highest M-QAM modulation used), weighted by the probability that the SNR γ falls in the nth region. The variable a_n is expressed as

$$a_n = \int_{\gamma_n}^{\gamma_{n+1}} p_\gamma(\gamma)\, d\gamma = \frac{\Gamma\left(m, \frac{m \times \gamma_n}{\bar{\gamma}}\right) - \Gamma\left(m, \frac{m \times \gamma_{n+1}}{\bar{\gamma}}\right)}{\Gamma(m)}, \tag{6.4}$$

where m is the Nakagami fading parameter, $\Gamma(\,)$ is the gamma function defined by $\Gamma(m) = \int_0^\infty y^{m-1} exp(-y) dy$, $\Gamma(.,.)$ is the incomplete gamma function defined by $\Gamma(x, a) = \frac{1}{\Gamma(a)} \int_0^x e^{-t} t^{a-1} dt$ and $\bar{\gamma}$ is the average SNR per symbol defined in (2.5) [22].

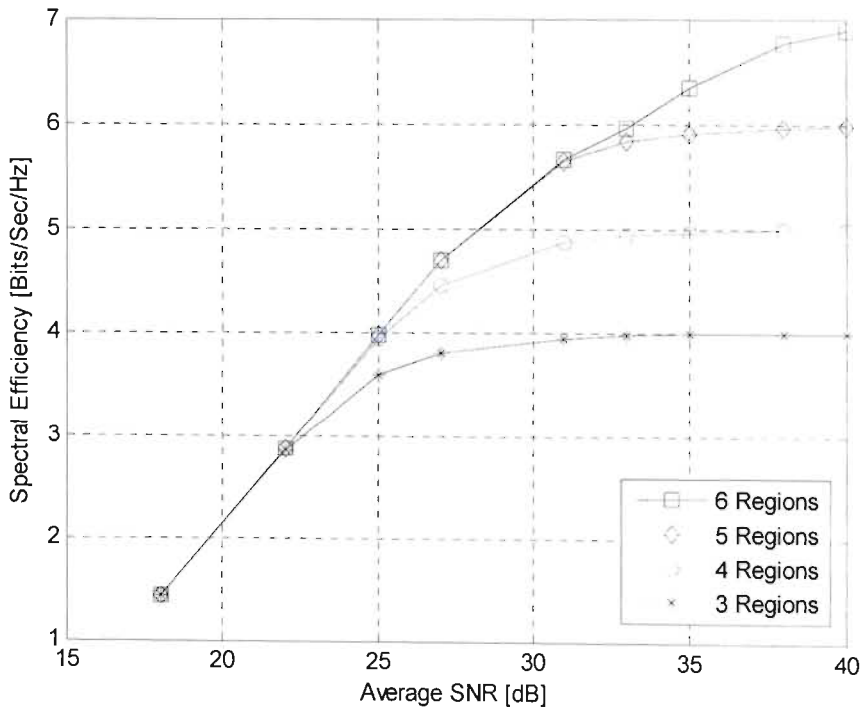

Figure 6-6: Spectral efficiency of M-QAM in an $m = 2$ Nakagami-m fading channel

Figure 6-6 shows the average link spectral efficiency of the adaptive M-QAM system at the physical layer for the $m = 2$ Nakagami-m fading channel with a BER target (BER_0) of 1×10^{-3}. The number of $N + 1$ regions in that 6 regions represents the use of 4-QAM to 128-QAM, 5 regions represents the use of 4-QAM to 64-QAM etc. As it would be expected, the graph shows that the average spectral efficiency reduces at the higher SNR regions as the number of regions decreases. The average link spectral efficiency of the physical and application layer cross-layer scheme is then determining by further multiplying the expression inside the summation in (6.4) with the RS code rate used in each SNR bin of the application layer for the three classes of traffic transmitted. The code rate for a particular application layer SNR bin can be determined from Table 6-2 to 6-4 for voice, video and data traffic, respectively. The average system link spectral efficiency, using 6 regions at the physical layer, RS(127, k) for voice traffic and RS(63, k) for video and data traffic at the application layer is shown in Figure 6-7, Figure 6-8 and Figure 6-9 for voice, video and data transmission respectively. As the graphs show, the spectral efficiency is reduced when compared to the uncoded physical layer adaptive M-QAM system and this is due to the insertion of the additional parity symbols at the application layer. The system spectral efficiency further reduces for video and data traffic when compared to voice traffic as the RS code rate is lower because a higher level of error protection is required for these two classes of traffic. The optimization of the system link spectral efficiency for the transmission of the three classes of traffic is left for future work.

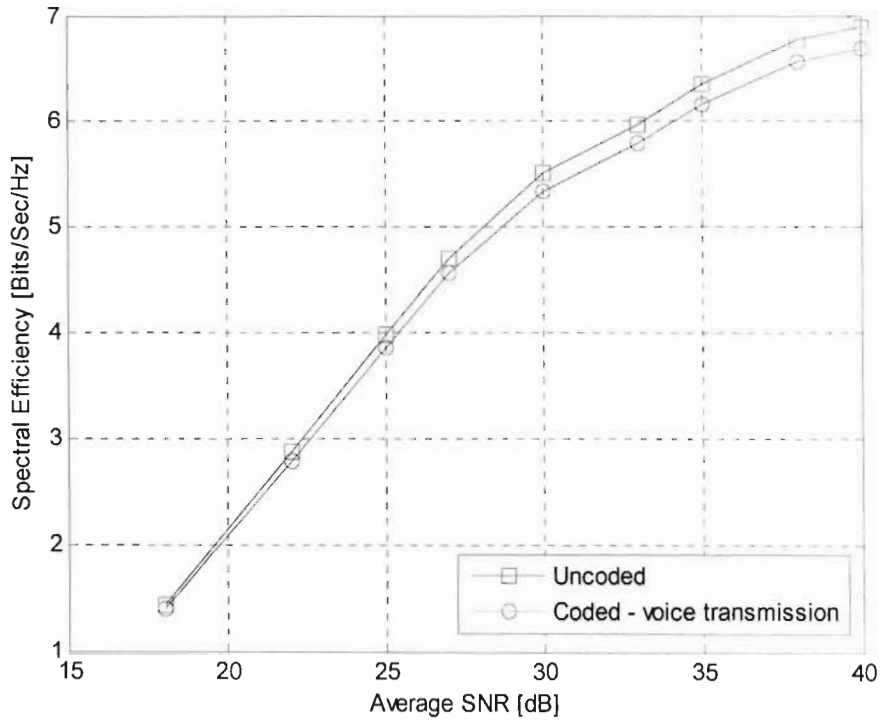

Figure 6-7: System spectral efficiency for the transmission of voice traffic in an $m = 2$ Nakagami-m fading channel

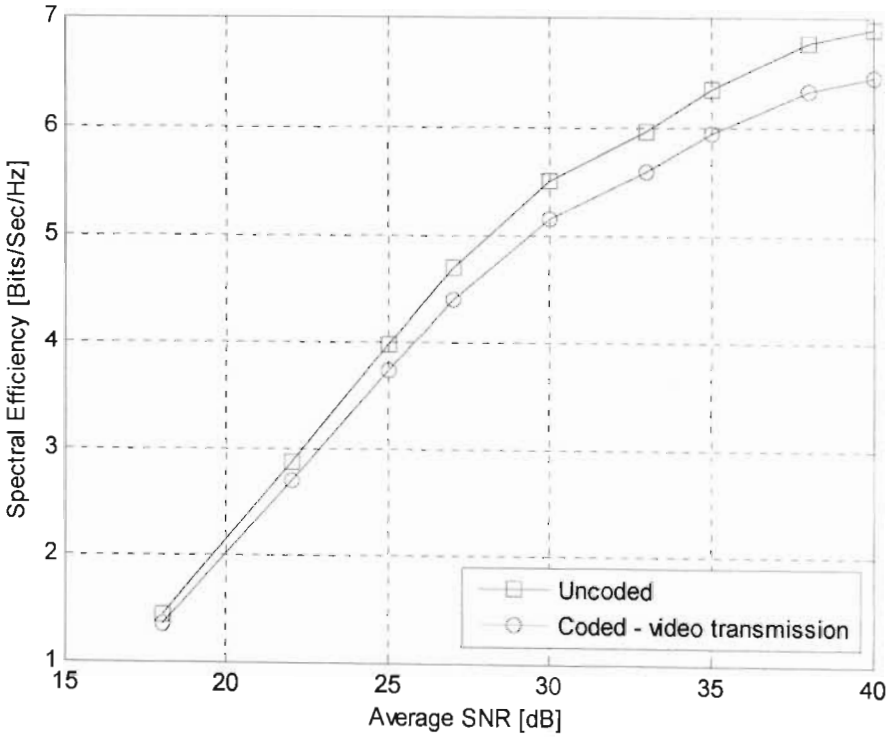

Figure 6-8: System spectral efficiency for the transmission of video traffic in an $m = 2$

Nakagami-m fading channel

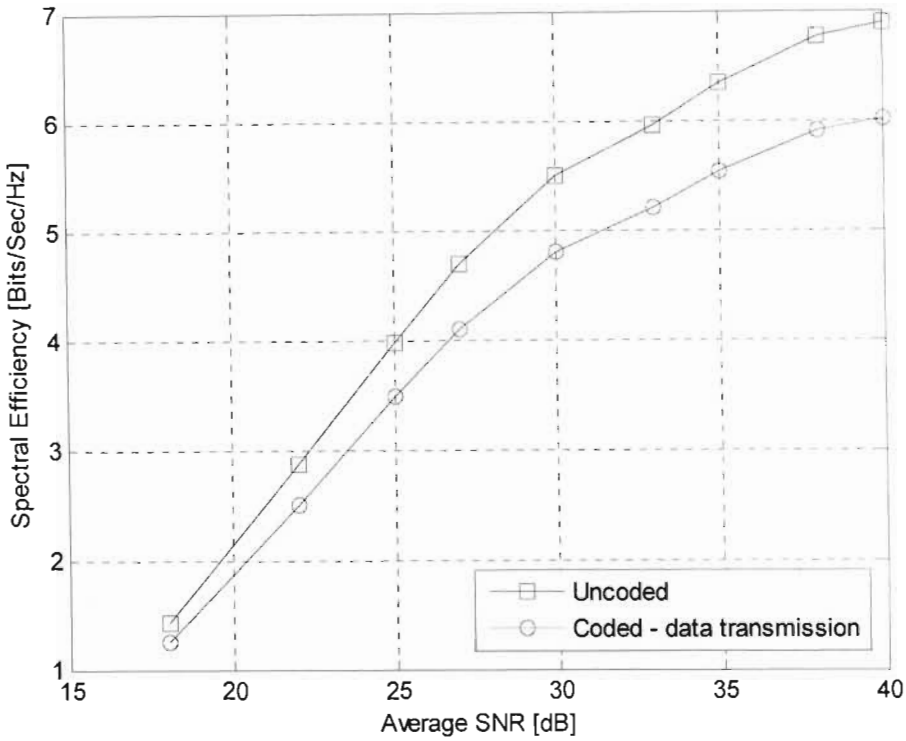

Figure 6-9: System spectral efficiency for the transmission of data traffic in an $m = 2$ Nakagami-m fading channel

6.4 Conclusion

In this chapter the system design of the physical and application layer cross-layer mechanism proposed in this thesis was modified for it to operate in a Nakagami-m channel. An accurate approximation average BER for M-QAM in a fading channel was used for the design of the adaptive M-QAM thresholds at the physical layer. The system theoretical performance, verified by simulations, showed that it meets its objective of guaranteeing error rate QoS targets for multiple classes of traffic in a single physical layer frame.

Chapter 7

Conclusion and Future work

Guaranteeing quality of service (QoS) for the transmission of multimedia traffic over wireless links has become essential if these applications are to receive wide spread acceptance. The challenges of providing QoS guarantees for multimedia traffic transmission over fading channels have been highlighted in this thesis. The limitation of the classical layered architecture in the communications structure was discussed and motivations for the cross-layer design methodology, in which the interdependence between interacting layers exploited for system optimization, was given. The application of cross-layer design for QoS provisioning was then discussed through examples of cross-layer schemes in dynamic resource allocation, scheduling and transmission of multimedia content over wireless links.

Many of the cross-layer mechanisms referenced, and the one proposed in this thesis, use a channel adaptive physical layer. An adaptive M-QAM has been commonly used because it is an efficient adaptive modulation method. However, much of the work that has applied this method uses the assumption that thresholds for adaptive M-QAM designed for AWGN channels can be directly applied to slowly varying block fading channels. These thresholds are calculated with a commonly used approximate BER expression in these schemes. The accuracy of the use of this commonly used expression in a fading channel was investigated by comparing the result of the average BER expression derived using the approximate expression with the results of simulations over a Nakagami-m block fading channel. The comparison of the results showed a significant difference (a gap of up to 4dB for 128-QAM) between the average BER computation and the simulation. Simulation results were also used to show that the inaccuracy in the threshold values determined using the closed form approximate BER expression will lead to inappropriate operation of the adaptive M-QAM scheme in a fading channel.

In order to improve the accuracy of the channel adaptive M-QAM system BER performance in a fading channel, the average BER over a Nakagami-m fading channel was re-derived using two alternative approximate BER expressions for M-QAM in AWGN. One of the average BER expressions was then used to determine the threshold values for the adaptive

Chapter 7

Conclusion and Future work

Guaranteeing quality of service (QoS) for the transmission of multimedia traffic over wireless links has become essential if these applications are to receive wide spread acceptance. The challenges of providing QoS guarantees for multimedia traffic transmission over fading channels have been highlighted in this thesis. The limitation of the classical layered architecture in the communications structure was discussed and motivations for the cross-layer design methodology, in which the interdependence between interacting layers exploited for system optimization, was given. The application of cross-layer design for QoS provisioning was then discussed through examples of cross-layer schemes in dynamic resource allocation, scheduling and transmission of multimedia content over wireless links.

Many of the cross-layer mechanisms referenced, and the one proposed in this thesis, use a channel adaptive physical layer. An adaptive M-QAM has been commonly used because it is an efficient adaptive modulation method. However, much of the work that has applied this method uses the assumption that thresholds for adaptive M-QAM designed for AWGN channels can be directly applied to slowly varying block fading channels. These thresholds are calculated with a commonly used approximate BER expression in these schemes. The accuracy of the use of this commonly used expression in a fading channel was investigated by comparing the result of the average BER expression derived using the approximate expression with the results of simulations over a Nakagami-m block fading channel. The comparison of the results showed a significant difference (a gap of up to 4dB for 128-QAM) between the average BER computation and the simulation. Simulation results were also used to show that the inaccuracy in the threshold values determined using the closed form approximate BER expression will lead to inappropriate operation of the adaptive M-QAM scheme in a fading channel.

In order to improve the accuracy of the channel adaptive M-QAM system BER performance in a fading channel, the average BER over a Nakagami-m fading channel was re-derived using two alternative approximate BER expressions for M-QAM in AWGN. One of the average BER expressions was then used to determine the threshold values for the adaptive

M-QAM system. Simulation results were then used to verify the accuracy of the new threshold points and the new average BER expression over the Nakagami-m fading channel.

The cross-layer design for QoS provisioning problem was then analysed more deeply, and it was noted that most of the schemes only focus on the interaction between lower (physical and data link) layers and ignore the possibility of sharing information with higher layers in the optimization process. One particular QoS provisioning cross-layer scheme is analysed and it is shown that this introduces functional and efficiency limitations which could be overcome if higher layers were incorporated. One such limitation that was discussed was the inability to insert more than one class of traffic in a physical layer frame. A novel cross-layer design which overcomes this limitation was then presented. The concept of unequal error protection was used to combine a channel adaptive coding scheme at the application layer to a channel adaptive physical layer in the design of the cross-layer scheme which will allow a resource allocation mechanism to insert three different classes of traffic, namely voice, video and data in a single physical layer frame. The cross-layer system was designed for the AWGN and a Nakagami-m channel and simulation results were used to show that it meets the objective of guaranteeing error rate QoS targets for all three classes of traffic in the operable signal-to-noise range.

The aim of future work will be to design an efficient cross-layer resource allocation scheme that will use the channel adaptive physical and application layer mechanism to guarantee other QoS metrics such as throughput and probability of delay violation. Also, one of the methods used to improve the system performance of wireless multimedia transmission systems is space diversity reception. The most prevalent space diversity combing techniques are maximal ratio (MR), equal gain (EG) and selection combining (SC). In order to reduce the complexity of such techniques switched diversity reception methods such as switch and stay combining (SSC) have been proposed. More recently, the concept of cooperative communications has been applied to the well known SSC technique where a single decode and forward (DF) relay is utilized to produce a virtual/distributed switch and stay combining (DSSC) system. The application of adaptive system studied in this thesis to improve the performance of a DSSC system in terms of throughput and delay violation will be part of future work.

Appendix I

Derivation of the integral for (2.6):

$$\int_0^\infty \gamma^{m-1} exp(-\gamma\beta) d\gamma$$

$$= \left(\frac{1}{\beta}\right)^{m-1} \int_0^\infty \gamma^{m-1} exp(-\gamma\beta)(\beta)^{m-1} d\gamma$$

$$= \left(\frac{1}{\beta}\right)^{m-1} \int_0^\infty (\gamma\beta)^{m-1} exp(-\gamma\beta) d\gamma$$

$$let\ \alpha = \gamma\beta, \quad d\gamma = \frac{1}{\beta} d\alpha$$

$$= \left(\frac{1}{\beta}\right)^{m-1} \int_0^\infty (\alpha)^{m-1} exp(-\alpha) \left(\frac{1}{\beta}\right) d\alpha$$

$$= \left(\frac{1}{\beta}\right)^{m} \int_0^\infty (\alpha)^{m-1} exp(-\alpha) d\alpha$$

$$= \left(\frac{1}{\beta}\right)^{m} \Gamma(m)$$

References

[1] van Der Schaar M., Sai Shankar N., "Cross-layer wireless multimedia transmission: challenges, principles, and new paradigms," *IEEE Wireless Communications*, vol. 12, no. 4, pp. 50-58, Aug 2005.

[2] Pajares A., Guerri J.C., Esteve M., Palau C., Leon A., Cardona N., "Dynamic frequency and resource allocation with adaptive error control based on RTP for multimedia QoS guarantees in wireless networks," IEEE International Conference on Multimedia Computing and Systems, 1999. vol. 2, pp. 333 – 337, Jun 1999.

[3] Huang L., Kumar S., Kuo C.-C.J., "Adaptive resource allocation for multimedia QoS management in wireless networks," *IEEE Transactions on Vehicular Technology*, vol. 53, no. 2, pp. 547 - 558, Mar 2004.

[4] Bourouha M., Ci S., Brahim G.B., Guizani M., "A cross-layer design for QoS support in the 3GPP2 wireless systems," IEEE Global Telecommunications Conference Workshops, 2004. GlobeCom Workshops 2004. pp. 56 – 61, Dec 2004.

[5] Jeong S.S., Jeong D. G., Jeon W. S., "Cross-layer Design of Packet Scheduling and Resource Allocation in OFDMA Wireless Multimedia Networks," IEEE 63rd Vehicular Technology Conference, 2006. VTC 2006-Spring. vol. 1, pp. 309 – 313, Mar 2006.

[6] Wang X., Liu Q., Giannakis G.B., "Analyzing and Optimizing Adaptive Modulation Coding Jointly With ARQ for QoS-Guaranteed Traffic," *IEEE Transactions on Vehicular Technology*, vol. 56, no. 2, pp. 710 - 720, Mar 2007.

[7] Lakshmanan P.K., Zeng Q., "Dynamic Adaptive Resource Allocation Scheme for Multimedia Services in Wireless and Mobile Networks," Wireless Telecommunications Symposium, 2006. WTS '06, pp. 1-7, Apr 2006.

[8] Huang L., Kumar S., Kuo C.-C.J., "Adaptive resource allocation for multimedia services in wireless communication networks," International Conference on Distributed Computing Systems Workshop, 2001. pp. 307-312, Apr 2001.

[9] Hui D. S. W., Lau V. K. N., Lam W. H., "Cross Layer Designs for OFDMA Wireless Systems with Heterogeneous Delay Requirements," IEEE International Conference on Communications, 2006. vol 12, pp. 5325 - 5330, Jun 2006.

[10] Wang W., Hwang K. C., Lee K. B., Bahk S., "Resource allocation for heterogeneous services in multiuser OFDM systems," IEEE Global Telecommunications Conference, 2004. GLOBECOM '04. Vol. 6, pp. 3478 - 3481, Dec. 2004.

[11] Tang J., Zhang X., "Cross-layer design of dynamic resource allocation with diverse QoS guarantees for MIMO-OFDM wireless networks," Sixth IEEE International

Symposium on a World of Wireless Mobile and Multimedia Networks, 2005. WoWMoM 2005. pp. 205-212, Jun 2005.

[12] Sun Z., Zhou Y., Peng M., Wang W., "Dynamic Resource Allocation with Guaranteed Diverse QoS for WiMAX System," International Conference on Communications, Circuits and Systems Proceedings, 2006. vol. 2, pp. 1347 - 1351, Jun 2006.

[13] Choi Y.-J., Bahk S., Lee K. B., "Wireless-adaptive fair scheduling for multimedia stream," *Electronics Letters*, vol. 39, no. 14, pp. 1093 - 1094, Jul 2003.

[14] Skyrianoglou D., Passas N., Salkintzis A., "Traffic scheduling for multimedia QoS over wireless LANs," IEEE International Conference on Communications, 2005. ICC 2005. vol. 2, Page(s):1266 - 1270, May 2005.

[15] Choi Y.-J., Bahk S., "WAF: wireless-adaptive fair scheduling for multimedia stream in time division multiplexed packet cellular systems," Eighth IEEE International Symposium on Computers and Communication, 2003. (ISCC 2003). Proceedings. pp. 1085 - 1090 vol.2. Mar 2003.

[16] Abd El-atty S.M., "Efficient Packet Scheduling with Pre-defined QoS using Cross-Layer Technique in Wireless Networks," 11th IEEE Symposium on Computers and Communications, 2006. ISCC '06. pp. 820 - 826, Jun 2006.

[17] Han Z., Liu X., Wang J., Liu K.J.R., "Delay sensitive scheduling schemes for heterogeneous QoS over wireless networks," *IEEE Transactions on Wireless Communications*, vol. 6, no. 2, pp. 423 - 428, Feb 2007.

[18] Liao D., Li L., "Traffic Aided Fair Scheduling Using Compensation Scheme in Wireless CDMA Networks," 6th International Conference on ITS Telecommunications Proceedings, 2006. pp. 802 – 807, Jun 2006.

[19] Zhu P., Zeng W., Li C., "Cross-Layer Design of Source Rate Control and Qos-Aware Congestion Control for Wireless Video Streaming," IEEE International Conference on Multimedia and Expo, 2006. pp. 1133 – 1136, Jul 2006.

[20] Peng Y., Khan S., Steinbach E., Sgroi M., Kellerer W., "Adaptive resource allocation and frame scheduling for wireless multi-user video streaming," IEEE International Conference on Image Processing, 2005. ICIP 2005. vol. 3, pp. 708 - 711, Sep 2005.

[21] Zhang Q., Zhu W., Zhang Y.-Q., "Channel-adaptive resource allocation for scalable video transmission over 3G wireless network", *IEEE Transactions on Circuits and Systems for Video Technology*, vol. 14, no. 8, pp. 1049 - 1063, Aug 2004.

[22] Alouini M. S., Goldsmith A. J., "Adaptive modulation over Nakagami fading channels," *Kluwer Journal on Wireless Communications*, vol 13, no. 1-2, pp 119-143,May 2000.

[23] Chen X., Chat C. C., Chew Y. H., "Performance of adaptive MQAM in cellular system Nakagami fading and log-normal shadowing", In Proceedings of IEEE Personal, Indoor and Mobile Radio Communications, 2003. PIMRC 2003, vol.2, pp: 1274 – 1278, Sept. 2003.

[24] Goldsmith A. J., Chua S.-G., "Variable-rate variable-power MQAM for fading channels", *IEEE Transactions on Communications*, vol 45, no 10, pp 1218-1230, Oct. 1997.

[25] Goldsmith A. J., Chua S.-G., "Adaptive coded modulation for fading channels", *IEEE Transactions on Communications*, vol 46, no 5, pp 595-602, May 1997.

[26] Hole K. J., Holm H., and Oien G. E., "Adaptive multidimensional coded modulation over flat fading channels," *IEEE Journal on Selected Areas in Communications*, vol.18, no. 7, pp. 1153–1158, Jul. 2000.

[27] Holm H., Hole K. J., Oien G. E., "Spectral Efficiency of Variable-Rate Coded QAM for flat fading channels", In Proceedings of Nordic Signal Processing Symposium *(NORSIG-99),* Asker, Norway, pp. 130 – 135, Sep. 1999.

[28] Hole K. J., Oien G. E., "Adaptive Coding and Modulation: A key to Bandwidth-Efficient Multimedia Communications in Future Wireless Systems". Invited paper, Telektronikk (special issue on "Wireless Future"), vol. 97, no. I, pp. 49 – 57, May 2001.

[29] Liu Q., Zhou S., Giannakis G. B, "A Cross-Layer Scheduling With Prescribed QoS Guarantees in Adaptive Wireless Networks", *IEEE Journal on Selected Areas in Communications*, vol 23, no 5, pp. 1056-1065, May 2005.

[30] Liu Q., Wang X., Giannakis G. B, "A Cross-Layer Scheduling Algorithm With QoS Support in Wireless Networks", *IEEE Transactions on Vehicular Technology*, vol 55, no 3, pp. 839-847, May 2006.

[31] Quazi T., Xu H., Takawira F., "Quality of Service for Multimedia Traffic using Cross-Layer Design", *IET Communications Journal*, vol 3, issue 1, pp 83-90, Jan. 2009.

[32] Yang H.-C., Belhaj N., Alouini M. S., "Performance Analysis of Joint Adaptive Modulation and Diversity Combining over Fading Channels", *IEEE Transactions on Communications*, vol 55, no 3, pp. 520- 528, Mar. 2007.

[33] Kim Y., Hwang G. U., "Performance Analysis of M-QAM Scheme Combined With Multiuser Diversity Over Nakagami-m Fading Channels", *IEEE Transactions on Vehicular Technology*, vol 57, no 5, pp. 3251-3257, Sep. 2008.

[34] Holter B., Oien G. E., "Performance Analysis of a Rate-Adaptive Dual-Branch Switched Diversity System", *IEEE Transactions on Communications*, vol 56, no 12, pp. 1998-2001, Dec. 2008.

[35] Gjendemsjo A., Yang H., Oien G.E, Alouini M. S. , "Joint Adaptive Modulation and Diversity Combining With Downlink Power control", *IEEE Transactions on Vehicular Technology*, vol 57, no 4, pp. 2145-2152, Sep. 2008.

[36] Nechiporenko T., Phan K.T., Tellambura C., Nguyen H.H, "Performance Analysis of Adaptive M-QAM for Rayleigh Fading Cooperative Systems", In Proceedings of IEEE International Conference on Communications, 2008. ICC '08, pp: 3393-3399, May 2008.

[37] Beaulieu N. C., Cheng C., "Efficient Nakagami-m Fading Channel Simulation", *IEEE Transaction on Vehicular Technology*, vol 54, no 2, pp 413-424, Mar. 2005.

[38] de Abreu G., "On the Simulation of Arbitrary Nakagami-m Channels", *IEEE Transactions on Vehicular Technology*, (conditionally accepted in March 2008).

[39] de Abreu G., "Accurate Simulation of Piecewise Continuous Arbitrary Nakagami-m Phasor Processes", Proceeding of IEEE Global Telecommunications Conference (GLOBECOMM '06), pp 1-6, Dec. 2006.

[40] Proakis J. G., *Digital Communications*, McGraw-Hill, Inc., New York, 2001.

[41] Simon M. K. and Alouini M. S., *Digital Communications over Fading Channels*, Wiley & Sons, Inc., New York, 2000.

[42] Al-Shahrani I., "Performance of M-QAM over Generalized Mobile Fading Channels using MRC Diversity", MSc Thesis, King Saud University, 2007.

[43] Chiani M., Dardari D., Simon M. K., "New exponential bounds and approximations for the computation of error probability in fading channels," *IEEE Transactions on Communications*, vol 2, no 4, pp. 840-845, Jul. 2003.

[44] Ci S., Guizani M., Benbrahim G., "A Dynamic Resource Allocation Scheme for Delay-Constrained Multimedia Services in CDMA 1xEV-DV Forward Link," *IEEE JSAC Special Issue on "Next Generation CDMA Technologies,"*, Vol. 24, No. 1, pp. 46-53, January 2006.

[45] Tang J., Zhang X, "Cross-Layer-Model Based Adaptive Resource Allocation for Statistical QoS Guarantees in Mobile Wireless Networks", *IEEE Transactions on Wireless Communications,* vol. 6, no. 12, pp. 4504-4512, Dec 2007.

[46] Johnsson K.B., Cox D.C., "An adaptive cross-layer scheduler for improved QoS support of multiclass data services on wireless systems", *IEEE Journal on Selected Areas in Communications*, Volume 23, Issue 2, pp. 334 – 343, Feb. 2005.

[47] Yu F., Wong V., Leung V., "Efficient QoS provisioning for adaptive multimedia in mobile communication networks by reinforcement learning", Proceedings of First International Conference on Broadband Networks, 2004. (BroadNets 2004). pp. 579 – 588, 25-29 Oct. 2004.

[48] Wu D., Negi R., "Effective Capacity: A wireless link model for support of quality of service", *IEEE Transactions on Wireless Communications*, vol. 2, no. 4, pp. 630-643, August 2003.

[49] Qiuyan X., Hamdi M., "Cross Layer Design for IEEE 802.11 WLANs: Joint Rate Control and Packet Scheduling", Proceedings of The IEEE Conference on Local Computer Networks, 2005. 30th Anniversary, pp. 624 – 631, 15-17 Nov. 2005.

[50] Chan Y., Cosman P., Milstein L. B., ``A Cross-Layer Diversity Technique for Multicarrier OFDM Multimedia Networks," *IEEE Transactions on Image Processing*, vol. 15, no. 4, pp. 833-845, April. 2006.

[51] Krishnamachari S., van der Schaar M., Choi S., and Xu X., "Video Streaming over Wireless LANs: A Cross-Layer Approach", in Proc. IEEE Packet Video '2003(PV '03), Nantes, France, April 2003.